

Reviewed Preprint

v1 • May 1, 2026

Not revised

✉ For correspondence:

michael.brunner@bzh.uni-heidelberg.de

Competing interests: No competing interests declared**Funding:** See page 30**Reviewing editor:** Volker Dötsch, Goethe University Frankfurt, Germany

© 2026, Serrano et al. This article is distributed under the terms of the [Creative Commons Attribution License](#), which permits unrestricted use and redistribution provided that the original author and source are credited.

Nuclear CK1 δ as a Critical Determinant of PER:CRY Complex Dynamics and Circadian Period

Fidel E Serrano, Daniela Marzoll, Bianca Ruppert, Axel CR Diernfellner, Michael Brunner ✉

Heidelberg University Biochemistry Center, Heidelberg, Germany

eLife Assessment

This **valuable** study examines the subcellular dynamics of the mammalian circadian clock proteins PER2, CRY1, and CK1, providing **solid** evidence that CK1 modulates the PER2-CRY1 interaction and drives the cytoplasmic localization of PER2 complexes. This could play a key role in modulating transcriptional repression by PER2, CRY1, and CK that contributes to the molecular circadian clock. There are minor concerns regarding the overexpression of the clock proteins in this study.

[Editors' note: this paper was previously reviewed by another journal.]

<https://doi.org/10.7554/eLife.110786.1.sa2>

Abstract

The mammalian circadian clock is governed by a feedback loop in which the transcription activator CLOCK:BMAL1 induces expression of its inhibitors, PERs and CRYs, which form a complex with CK1 δ , the main circadian kinase. However, the spatiotemporal dynamics of this feedback loop and the precise role of CK1 δ remain incompletely understood. Using an inducible overexpression system, we show that nuclear availability of CK1 δ is limited by both rapid nuclear degradation and active export of unassembled kinase, while cytoplasmic kinase is readily available for association with PERs. We demonstrate that CK1 δ -mediated phosphorylation may disrupt PER2-CRY1 interaction thereby resulting in cytoplasmic PER2 dimers containing substoichiometric amounts of CRY1. Analysis of endogenous PER2 localization in the context of an intact circadian clock reveals that PER2 accumulates in the cytoplasm late in the circadian cycle. Based on these findings, we propose that cytoplasmic accumulation of PER:CRY:CK1 δ complexes contributes to the clearance of nuclear PER2, while the CK1 δ -dependent release of CRY1 into the nucleus may sustain CLOCK:BMAL1 repression on DNA supporting the transition from the early to the late repressive phase.

Introduction

Circadian clocks are molecular oscillators that regulate 24 h physiological rhythms as an adaptive response to day-night cycles^{1,2}. In mammals, the core clock relies on a delayed negative transcription-translation feedback loop (TTFL), in which the transcriptional activators BMAL1 and CLOCK drive the expression of their inhibitors, PERIOD (PER) and CRYPTOCHROME (CRY) proteins³⁻⁵. This core loop is reinforced by a secondary feedback loop in which the nuclear receptors RORs and REV-ERBs connect the core oscillator to cellular metabolism by activating and repressing *BMAL1* transcription, respectively^{6,7}. Circadian clocks are expressed in many tissues and entrained by daily recurring cues. Entraining environmental light cues are received by the suprachiasmatic nucleus (SCN), which directly and indirectly synchronizes clocks in peripheral organs via neuronal and hormonal/humoral cues. Recurring metabolic cues entrain peripheral clocks in the liver and other organs and determine their phase relative to the 24-hour light-dark cycle. The circadian system directly and indirectly controls key metabolic pathways⁸⁻¹⁰.

The prevailing “dual-mode of circadian repression” model offers a robust framework for understanding the circadian clock on the molecular level, distinguishing between the so-called “early” and “late” repressive phases. During the early repressive phase, a complex composed of PERs, CRYs, and casein kinase 1 δ (CK1 δ) assembles on CLOCK:BMAL1, leading to CLOCK phosphorylation, reducing CLOCK:BMAL1 binding to DNA, and thereby resulting in “displacement”-type repression. In the late repressive phase, phosphorylated PER proteins are degraded and the remaining CRY1 directly suppresses CLOCK:BMAL1 by sequestering the BMAL1 transactivation domain (TAD) resulting in “blocking”-type repression. Upon CLOCK dephosphorylation, the CLOCK:BMAL1 complex re-associates with DNA, establishing a poised promoter state. This configuration is characterized by transcriptional readiness, awaiting CRY1 to decrease below a threshold allowing reinitiation the circadian transcriptional cycle^{11–17}. It has been shown recently that CLOCK:BMAL1 in the SCN remains partially repressed by CRY1 even at peak circadian transcription¹⁸, a mechanism that may ensure responsiveness of the circadian clock to synchronizing cues^{18,19}.

Clock component homologs generally have redundant functions but differ in expression phases and binding affinities. PER1 and PER2 are both essential for maintaining robust circadian rhythms. PER1, expressed earlier, shortens the circadian period when PER2 is absent, whereas PER2 lengthens the period when PER1 is absent; PER3 plays a less critical role^{20,21}. CRY1 and CRY2 exhibit overlapping repressive functions when complexed with PER proteins. In addition, CRY1, but not CRY2, serves as a potent repressor of CLOCK:BMAL1 after PERs are degraded^{3,22,23}. As a consequence, CRY1 lengthens and CRY2 shortens circadian period²³. The casein kinase 1 splice isoforms CK1 δ 1 and CK1 δ 2, and the similar CK1 ϵ all support the clock, with their contributions varying potentially by tissue-specific expression^{24,25}. Likewise, NPAS2 can partially substitute for CLOCK in a tissue-specific manner²⁶.

PER proteins serve as limiting scaffolds for the assembly of the repressive complex, playing a key role in circadian timing. CK1 δ is crucial in regulating PER stability and function by phosphorylating PER proteins at numerous sites. A central aspect of this regulation involves the phosphorylation of hPER2 at S662 (S659 in mPer2) within the FASP (Familial Advanced Sleep Phase) region by CK1 δ bound to the Casein Kinase Binding Domain (CKBD)^{27,28}. This priming phosphorylation triggers rapid phosphorylation of four additional equally spaced residues in the FASP region. When fully phosphorylated, the FASP region inhibits CK1 δ by blocking its active site²⁹. This attenuation slows the phosphorylation of hPER2 S478 (S475 in mPer2), a residue within the β -TrCP phosphodegron, thereby delaying PER2 degradation, which is thus aligned with the circadian time frame³⁰. This so-called “phosphoswitch” mechanism is well-characterized, involving the phosphorylation of five residues in the FASP region and one in the β -TrCP degron of PER2^{30–32}. Phosphorylation of the FASP and β -TrCP regions severely impacts circadian period length but is not essential for circadian clock function per se. PER proteins are subjected to extensive hyperphosphorylation at numerous additional sites (about 80 in PER2) distributed across the protein³³. The kinetics of this widespread hyperphosphorylation strongly correlate with circadian timekeeping³⁴, but the functional significance of these modifications remains largely unknown. While it has been shown that phosphorylation of mPER1 masks an NLS³⁵, the potential impact of PER phosphorylation on subcellular localization and interaction with other proteins has not been systematically analyzed. Furthermore, CK1 δ is the main circadian kinase but is implicated in other essential cellular functions including regulation of the cell cycle and Wnt signalling^{36,37}. The regulation, subcellular distribution, and functional allocation of CK1 δ to its various tasks have yet to be fully elucidated.

Circadian proteins are expressed at relatively low physiological levels with many studies analyzing endogenous proteins contributing to our current understanding of the clock^{15,38–44}. To complement these studies and gain additional mechanistic insight, we utilized an inducible cellular overexpression approach combined with time-lapse live-cell imaging to investigate the dynamic interactions and subcellular localizations of CK1 δ , PER2, and CRY1 without interference from their endogenously expressed specific binding partners. Our findings reveal that PER2 and CRY1 mutually influence their stability, as well as their nuclear-cytoplasmic shuttling dynamics

and equilibrium. We demonstrate that CK1 δ turnover and shuttling are modulated in a kinase activity-dependent manner such that free active nuclear CK1 δ is rapidly degraded, making it a limiting factor for interactions with nuclear PER2. In contrast, CK1 δ is readily available in the cytosol. Phosphorylation of PER2 by CK1 δ drives, with a delay, PER2 cytosolic localization and, interestingly, disrupts PER2-CRY1 interaction. Translocation of the released CRY1 into the nucleus could then contribute to blocking-type repression of CLOCK:BMAL1.

Results

PER2 and CRY1 mutually affect their subcellular shuttling dynamics

To investigate the shuttling dynamics and subcellular localization of PER2, CRY1, and PER2:CRY1 complexes, we tagged PER2 at its C-terminus with mNeonGreen (PER2-mNG) and CRY1 at its N-terminus with mKate2 (mK2-CRY1) (Fig. EV1A [↗](#)). Proteins were expressed under the control of a doxycycline (DOX)-inducible CMV promoter in U2OStx cells harboring a TET repressor (Life Technologies, R712-07), either via transient transfection or in stable cell lines, depending on the experimental setup. This inducible overexpression strategy was deliberately chosen, as tagging and expressing the proteins at endogenous levels from their native loci would not have been suitable for addressing the questions examined in this study as specified below. PER2 contains a nuclear localization signal (NLS) and three CRM1-dependent nuclear export signals (NESs). It shuttles between the cytosol and nucleus and CRY1 facilitates its nuclear accumulation^{38,40,45,46}. However, analyzing the shuttling dynamics of PER2 alone is more complex than it might initially seem, as overexpression of PER2 stabilizes and thereby supports the accumulation of endogenous CRY proteins^{47,48}. Thus, analysis of PER2 localization at steady state⁴⁰ or at late time points after transient expression⁴⁵ likely reflect the localization of PER2:CRY complexes. We reasoned that inducing a burst of PER2 overexpression from a strong promoter would initially outcompete the cellular capacity to sufficiently accumulate endogenous CRYS. Time-resolved analysis would then allow for the characterization of PER2 shuttling dynamics before it quantitatively engages with endogenous CRYS, up to the point at which a subcellular steady state of PER2:CRY complexes is established.

In order to induce a sharp burst of PER2 overexpression, non-confluent U2OStx cells were transiently transfected with PER2-mNG. The cells were then grown for 24 h without induction in order to provide a time window for the cell cycle-dependent nuclear uptake of the transfected DNA. Subsequent DOX-induction triggered the intended sharp burst of PER2-mNG expression. The dynamics of the subcellular localization of PER2-mNG was then analyzed at 4 h intervals over a time period of 28 h by live-cell microscopy using an Incucyte (Sartorius) system. A representative time course of the subcellular shuttling dynamics of overexpressed PER2-mNG upon DOX induction is shown in Fig 1A [↗](#). Four hours after DOX induction, PER2-mNG localized predominantly to the cytosol and gradually shifted to the nucleus over a period of approximately 28 hours (Fig 1A [↗](#), upper panels). When CRM1-dependent nuclear export was inhibited with leptomycin B (LMB), PER2-mNG rapidly accumulated in the nucleus (Fig 1A [↗](#), lower panels), indicating that PER2 alone undergoes rapid nucleocytoplasmic shuttling. Immunoblot analysis revealed that DOX-induced overexpression of either transiently transfected PER2-mNG or stably-integrated V5-PER2 led to increased levels of endogenous CRY1 (Fig 1B, C [↗](#)). Considering that the transfection efficiency of U2OStx cells with PER2-mNG is low (<20%), the induction of endogenous CRY1 in the transiently transfected cells was substantial. The slow nuclear accumulation of PER2-mNG correlated with expression levels of endogenous CRY1, consistent with CRY1's role of promoting PER2 nuclear localization⁴⁶. These data demonstrate that PER2 alone shuttles rapidly between nucleus and cytoplasm. Its predominant cytoplasmic localization prior to the accumulation of endogenous CRYS indicates that the nuclear export of PER2 is substantially faster than its nuclear import. The nuclear accumulation dynamics of PER2 correlates with the PER2-

dependent accumulation of endogenous CRY1. Hence, the apparently slow export of overexpressed PER2 determined previously at steady state⁴⁰ likely reflects the shuttling dynamics of PER2 that is in complex with endogenous CRYs.

To examine how PER2 and CRY1 influence each other's subcellular dynamics, it was necessary to vary their expression levels independently while excluding contributions from endogenous PER1 and CRY2. This can only be achieved through transient transfection, as no system currently allows systematic manipulation of PER2 and CRY1 expression ratios at their endogenous loci. Although transient overexpression results in PER2 and CRY1 levels vastly exceeding those of their endogenous binding partners (i.e., PER1, CRY2, and CK1 δ/ϵ), the overall expression levels are not high enough to saturate transient interactions with nuclear transport or degradation pathways. Therefore, U2OS_{tx} cells were transfected with PER2-mNG and mK2-CRY1 either separately or together at different ratios and, after 24 h, expression was induced with DOX. The dynamics of the subcellular localization and interaction (colocalization) of PER2-mNG and mK2-CRY1 was analyzed at 4 h intervals over a time period of 28 h (Fig 1D [↗](#)). Transient expression of mK2-CRY1 alone was observed after 4 h, with the protein localizing to the nucleus and remaining nuclear until it was degraded around 28 h post-DOX induction (Fig 1D [↗](#), upper row). When PER2-mNG and mK2-CRY1 were coexpressed, the subcellular dynamics and expression pattern varied depending on their expression ratio (Fig 1D [↗](#) and EV1B [↗](#)). At a 1:3 transfection ratio of PER2-mNG : mK2-CRY1 (Fig 1D [↗](#), 2nd row), mK2-CRY1 was nuclear at all times, and nuclear accumulation of PER2-mNG was accelerated, as previously reported.⁴⁶ PER2-mNG and mK2-CRY1 accumulated in nuclear foci, which progressively decreased in number while increasing in size over time. The foci formed by the overexpressed clock proteins will be briefly characterized and discussed below. At a 1:1 transfection ratio (Fig 1D [↗](#), 3rd row), PER2-mNG accumulated in the nucleus more slowly, where it formed foci with mK2-CRY1. At early time points (4 h and 8 h) some mK2-CRY1 colocalized with PER2-mNG in the cytosol. At a 3:1 ratio (Fig 1D [↗](#), 4th row), nuclear accumulation of PER2-mNG was slow and a substantial fraction of mK2-CRY1 colocalized with PER2-mNG in the cytosol for up to 16 h. PER2-mNG by itself localized 4 h after DOX-induction predominantly in the cytosol and slowly relocated to the nucleus over a time course of about 20 h (Fig 1D [↗](#), bottom row), which correlates with the accumulation of endogenous CRYs (see Fig 1B, C [↗](#)). Since PER2-mNG alone accumulates in the cytosol and mK2-CRY1 alone is nuclear, the data indicate that PER2 and CRY1 mutually influence each other's nucleocytoplasmic shuttling dynamics and subcellular distribution. PER2 forms dimers and can therefore bind either one or two CRY1 molecules. Hence, at high mK2-CRY1 levels and/or at late timepoints after DOX induction, nuclear PER2-mNG:mK2-CRY1 complexes likely represent dimers fully saturated with two mK2-CRY1 molecules. Conversely, the prolonged cytosolic presence of mK2-CRY1 at low co-transfection ratios can only be explained by partially saturated complexes, in which a PER2-mNG dimer is bound to a single mK2-CRY1. Together, these findings indicate that the relative abundance and concentration, and thus, the degree of saturation, of dimeric PER2-mNG with monomeric mK2-CRY1 governs the balance between nuclear import and export kinetics of PER2:CRY1 complexes. Given that PER2 is predominantly cytosolic and free CRY1 is primarily nuclear, and that CRY1 promotes the nuclear accumulation of PER2, our findings suggest that CRY1 can remain in the cytosol only when incorporated into asymmetric, partially saturated complexes (Fig 1E [↗](#)). The potential physiological relevance of such complexes will be discussed below in light of recent quantifications of cytosolic PER2 and CRY1 in SCN slices across the circadian cycle.¹⁸

PERs and CRYs in nuclear foci retain their interaction specificity

The data shown above demonstrate that clock proteins have the capacity to engage in higher molecular mass assemblies. While the formation of large, thermodynamically persisting nuclear foci is clearly a consequence of overexpression, smaller assemblies may form dynamically and transiently under physiological conditions. In the context of our work, however, the foci are a convenient tool for easily analyzing the colocalization of clock proteins. To characterize the foci formed by the overexpressed clock proteins, a stable U2OS_{tx}_mK2-CRY1 line was transfected with untagged PER2 to induce formation of nuclear foci (Fig 2A [↗](#)). Since all cells express mK2-CRY1 and the transfection efficiency of U2OS_{tx} cells with PER2 is relatively low, the majority of cells

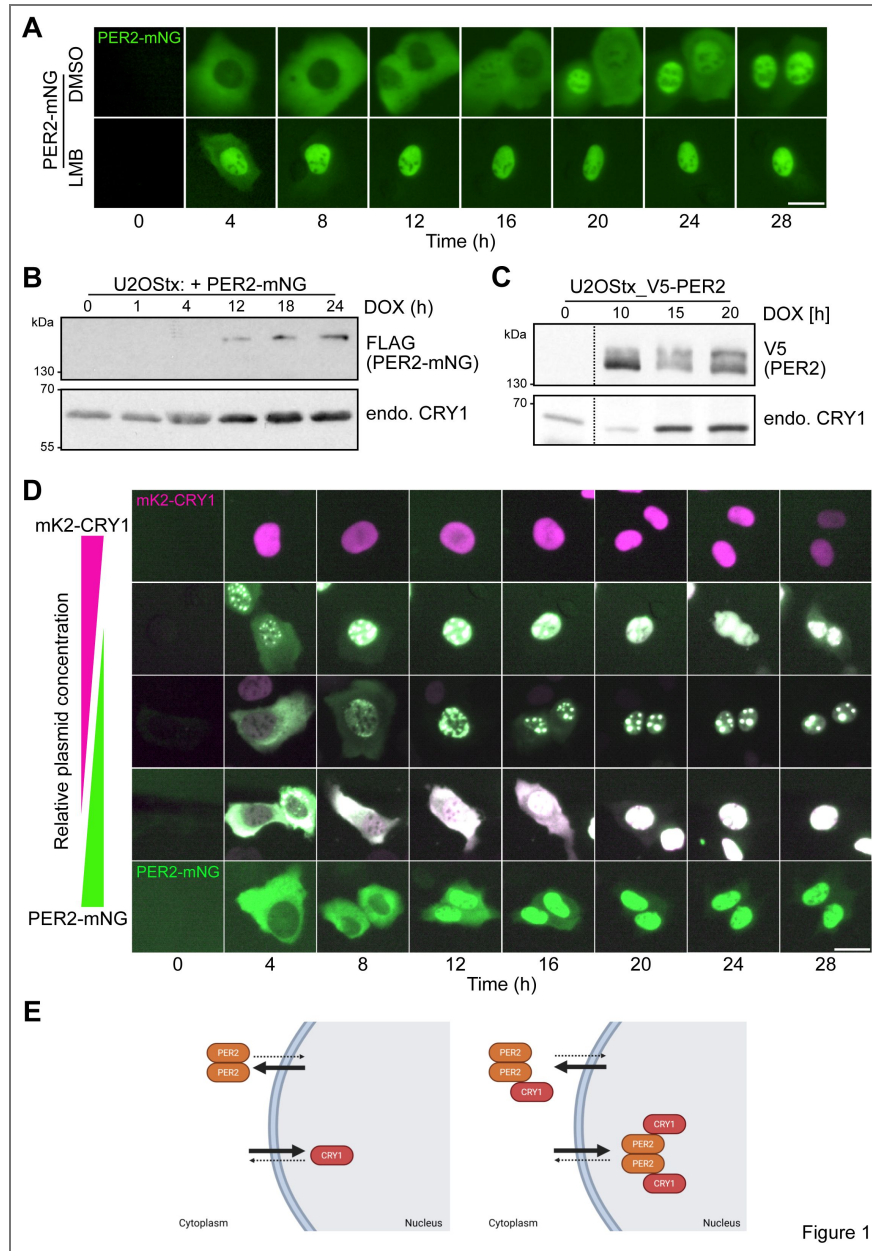


Figure 1

Fig 1. Subcellular dynamics of overexpressed PER2 and CRY1

(A) PER2-mNG exhibits rapid nucleocytoplasmic shuttling with a preference for the cytoplasm at early timepoints. DOX-induced expression of PER2-mNG in absence (DMSO) and presence of LMB. Scale bar 25 μ m. n = 3. (B) Expression of PER2-mNG supports accumulation of endogenous CRY1 with kinetics correlating with nuclear accumulation of PER2-mNG. Western blot analysis of U2OS cells transiently transfected and DOX-induced with PER2-mNG sampled at various time points post-DOX induction. (The accumulation of endogenous CRY1 in PER2-mNG-transfected cells is much higher than it appears because the transfection efficiency of U2OS cells is <20%.) n = 3. (C) Induction of stably-integrated V5-PER2 supports accumulation of endogenous CRY1 with kinetics correlating with nuclear accumulation of PER2-mNG. Western blot analysis of V5-PER2 and CRY1 from DOX-induced U2OS_V5-PER2 cells at the indicated time points post induction. n = 3. (D) CRY1 and PER2 mutually affect their subcellular dynamics and localization. DOX-induced transiently expressed mK2-CRY1 (top row) and PER2-mNG (bottom row) individually and in combination was analyzed over 28 h. Co-expression was assessed at mK2-CRY1 : PER2-mNG ratios of 3:1 (second row), 1:1 (third row), and 1:3 (fourth row). Scale bar 25 μ m. n = 3. (E) Model of subcellular localization of PER2, CRY1, and PER2:CRY1 complexes based on their relative stoichiometries. Left: PER2 dimers, which undergo rapid nuclear–cytoplasmic shuttling, are predominantly localized in the cytoplasm, whereas CRY1 is mainly nuclear. Right: PER2 dimers bound to a single CRY1 molecule remain mainly cytoplasmic, while PER2 dimers bound to two CRY1 molecules localize to the nucleus.

displayed a homogenous nuclear distribution of mK2-CRY1 while fewer cells accumulated mK2-CRY1 in nuclear foci (Fig 2B [↗](#) and EV2A [↗](#)). Immunofluorescence (IF) with PER2 antibodies confirmed that overexpressed PER2 colocalized with mK2-CRY1 in nuclear foci while endogenous PER2 exhibited diffuse cellular localization in mK2-CRY1 expressing cells without foci. Further IF analysis revealed that endogenous PER1, BMAL1, and CK1 δ 1 colocalized in these nuclear foci (Figs 2C-E [↗](#)) in contrast to their dispersed subcellular distribution in cells that contained no foci (Fig EV2B-D [↗](#)). Notably, PER1, BMAL1 and CK1 δ expression levels were elevated in cells containing nuclear PER2 and mK2-CRY1 foci compared to neighboring cells that remained untransfected with PER2-mNG (Fig 2C-E [↗](#)). The data suggest that overexpressed PERs and CRYs have the capacity to form nuclear foci where they maintain specific interactions with other clock proteins and support their accumulation at elevated levels. Particularly interesting was the PER2-dependent accumulation of CK1 δ at elevated levels, given that little is known about how kinase expression is regulated.

CK1 δ stability is regulated in an activity-dependent manner

To directly study the regulation of CK1 δ and the impact of PER2, we used previously generated stable U2OStx cell lines expressing the C-terminally FLAG-tagged wild-type CK1 δ 1 isoform, the tau-like mutant kinase CK1 δ 1-R178Q, and the kinase-dead version CK1 δ 1-K38R³⁴. Upon DOX induction, mRNAs of the induced transgenes were expressed at similar levels, approximately 50-fold higher than the endogenous CK1 δ RNA (Fig 3A [↗](#)). However, the proteins were expressed at vastly different levels (Fig 3B [↗](#)). CK1 δ 1 was expressed at the lowest level, CK1 δ 1-R178Q at an intermediate level, and CK1 δ 1-K38R at the highest level, suggesting an inverse correlation between resulting expression level and kinase activity or substrate specificity. Immunoblot analysis using a CK1 δ -specific antibody (Fig EV3A [↗](#)) revealed that, in the absence of DOX, the FLAG-tagged kinases were leakily expressed at levels comparable to endogenous CK1 δ (Fig 3B [↗](#), bottom panel). Upon DOX induction, the FLAG-tagged kinases were overexpressed. We then tested whether the differences in resulting kinase expression were due to protein turnover. Following a cycloheximide (CHX) chase, overexpressed CK1 δ 1 was rapidly degraded with a half-time of less than 15 min, whereas CK1 δ 1-K38R and CK1 δ 1-R178Q remained stable (Fig 3C, E [↗](#)).

When U2OStx control cells were treated with CHX, endogenous CK1 δ remained stable over the 90 min course (Fig 3D, E [↗](#)), consistent with previous studies^{3,11}. These data suggest that CK1 δ is rapidly degraded only when overexpressed, a process facilitated by its enzymatic activity. In contrast, endogenous CK1 δ , expressed at much lower physiological levels, may remain stable through interactions with various client proteins that protect it from degradation. To displace endogenous CK1 δ from potential binding sites, we overexpressed CK1 δ 1-FLAG or mNG-CK1 δ 1. Overexpression of either kinase markedly reduced endogenous CK1 δ levels, suggesting exchange between kinase-interacting partners and degradation of unbound kinases (Fig EV3B, C [↗](#)).

Since the mutant kinases CK1 δ 1-R178Q and CK1 δ 1-K38R were stable and expressed at higher levels than CK1 δ 1, we investigated how pharmacological inhibition with PF670462 (hereafter referred to as PF670), a well-characterized inhibitor of CK1 δ ⁴⁹, affects the expression of both endogenous and overexpressed CK1 δ 1. Treatment with PF670 for 1 h stabilized overexpressed CK1 δ 1 but, consistent with previous reports⁵⁰, did not affect the abundance of endogenous CK1 δ in U2OStx control cells (Fig 3F [↗](#)). Our data suggest that enzymatically active, overexpressed CK1 δ 1 is rapidly degraded, likely because it is not assembled with client proteins. CK1 δ is degraded by the proteasome via the APC/C-Cdh1 ubiquitin ligase⁵¹. To further characterize the degradation pathway of CK1 δ , we treated cells with the proteasome inhibitor MG132 (Fig 3G [↗](#)). In cells overexpressing CK1 δ 1, a 4 h treatment with MG132 led to a significant increase in CK1 δ 1 abundance, indicating that, in the absence of MG132, a large fraction of CK1 δ 1 synthesized from overexpressed RNA was degraded. CK1 δ 1-K38R was also stabilized by MG132 but to a lesser extent. In contrast, MG132 treatment of U2OStx control cells did not increase endogenous CK1 δ levels within the 4 h time frame.

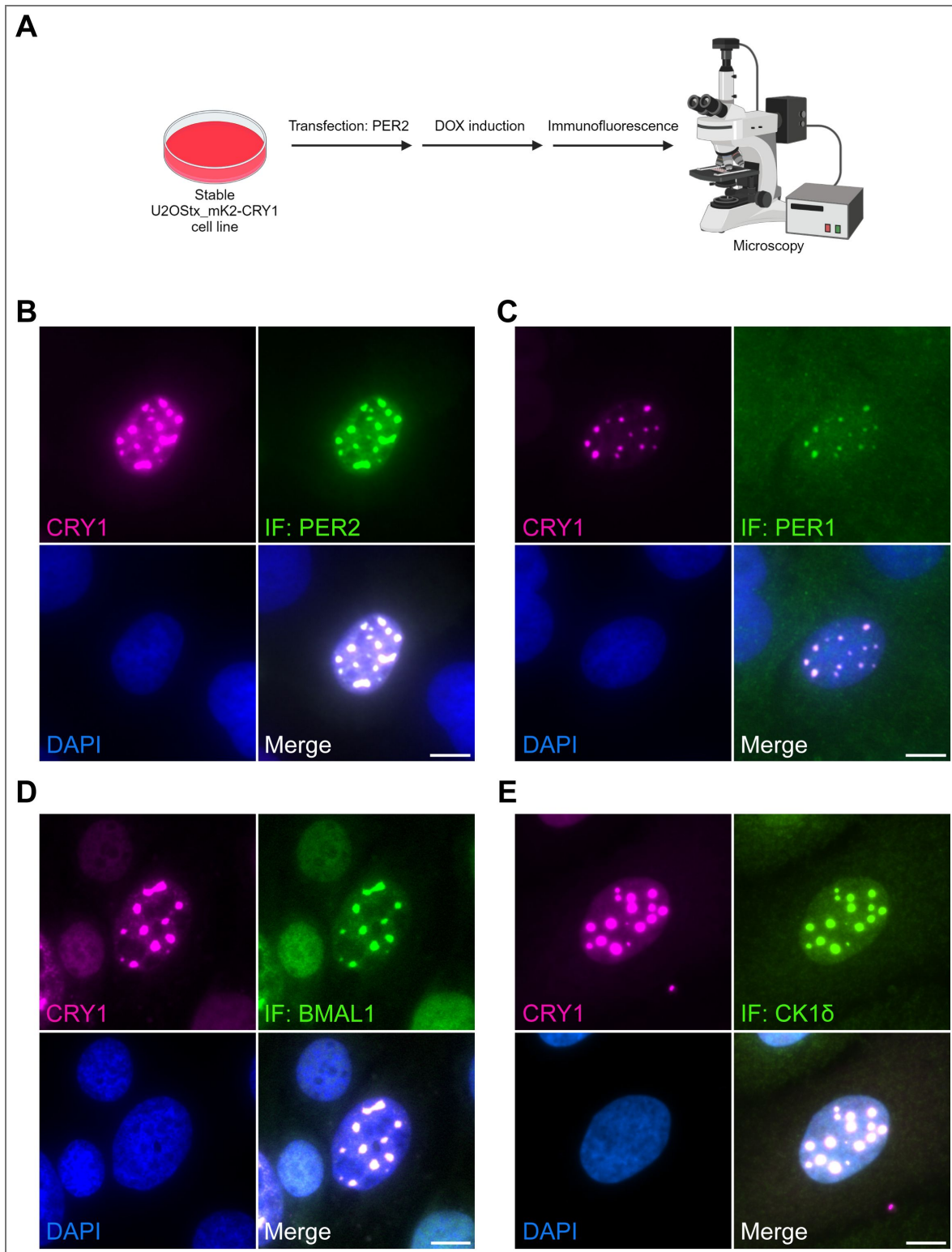


Fig 2. PERs and CRYs in nuclear foci retain their interaction specificity

(A) Schematic of the experimental setup: U2OSStx_mK2-CRY1 cells were transfected with PER2 and induced with DOX. Cells were analyzed for mK2-CRY1 expression and by immunofluorescence (IF) using specific antibodies. (B) IF for PER2: mK2-CRY1 and PER2 co-accumulate in nuclear foci. (C) IF for PER1: nuclear foci contain endogenous PER1. (D) IF for BMAL1: nuclear foci contain endogenous BMAL1. (E) IF for CK1δ: nuclear foci contain endogenous CK1δ. Expression levels of endogenous clock proteins are elevated in transfected cells compared to surrounding untransfected cells. Scale bars: 10 μ m. n = 3.

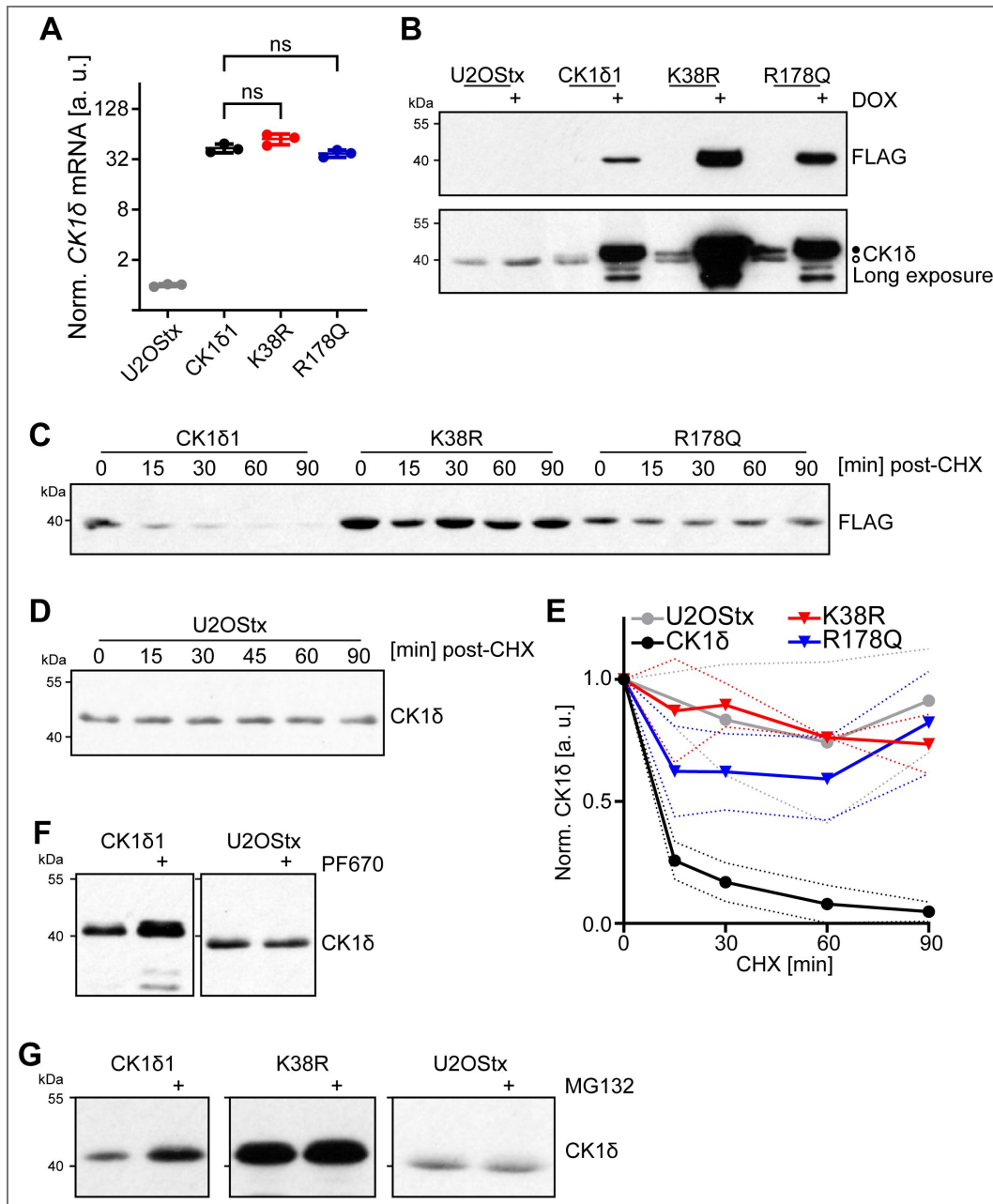


Fig 3. CK1δ is stability regulated in an activity-dependent manner

(A) qPCR analysis of *CK1δ* mRNA in U2OSStx cells and stable U2OSStx cell lines expressing DOX-inducible CK1δ1, CK1δ1-K38R, and CK1δ1-R178Q. n = 3, Students t-test, ns: not significant. n = 3. (B) Immunoblot analysis of DOX-induced CK1δ variants. Upper panel: DOX-induced expression of indicated FLAG-tagged CK1δ1 variants in stable U2OSStx cell lines. Lower panel: Expression of endogenous CK1δ (open circle) and CK1δ1-FLAG variants (filled circle) analyzed with an antibody detecting CK1δ1 and CK1δ2 but not CK1ε (Figure EV2). n = 3. (C) Overexpressed CK1δ1 is unstable with a half-life of about 6 min. CK1δ1-K38R and CK1δ1-R178Q are stable over 90 min. U2OSStx_CK1δ1 cells were DOX-treated for 24 h and then treated with CHX. Samples were collected after the indicated time periods (CHX chase) and analyzed by immunoblotting with FLAG antibody. (D) Endogenous CK1δ is stable over 90 min post CHX chase. (E) Quantification of (C) and (D). n = 3, solid and dashed lines: mean ± SD. (F) Left panel: Inhibition by PF670 stabilizes overexpressed FLAG-tagged CK1δ1. Right panel: 1h PF670 treatment of control cells has no effect on endogenous CK1δ levels. More protein (4x) was loaded on the gel for the analysis of endogenous CK1δ. n = 3. (G) Proteasomal inhibition by MG132 (4 h) stabilizes overexpressed (left panel) CK1δ1 and, (middle panel) to a lesser extent, the already stable CK1δ1-K38R. Right panel: MG132 has no effect on endogenous CK1δ levels in U2OSStx control cells within the 4 h treatment window. n = 3.

These findings suggest that the high levels of CK1 δ 1 produced from abundant DOX-induced mRNA are rapidly degraded in a kinase activity-dependent manner, presumably because the kinase is not assembled with client proteins. Due to the high synthesis rate of the overexpressed CK1 δ 1, a 1 h inhibition of kinase activity with PF670 or a 4 h inhibition of protein turnover with MG132 was sufficient to raise CK1 δ 1 level to a detectable extent. In contrast, in control cells, the translation of the 50-fold less abundant endogenous CK1 δ RNA (Fig 3A) was not sufficient to significantly increase kinase expression beyond the steady-state level within the inhibitor treatment time windows (Fig 3F, G). The data suggest that free CK1 δ is present at low levels, potentially acting as a limiting factor for interactions with partners such as PER proteins.

PER2 supports accumulation of endogenous CK1 δ

To investigate whether the expression of PER2, a binding partner of CK1 δ , is sufficient to elevate endogenous CK1 δ levels, we generated stable U2OStx cell lines that overexpress V5-tagged PER2 in a DOX-dependent manner. Upon induction of PER2 expression, similar to endogenous CRY1 (see Fig 1B, C), endogenous CK1 δ 1 levels increased in parallel with PER2 requiring several hours for a detectable accumulation of the endogenous kinase (Fig 4A). The data suggest that PER2 acts as a stabilizing binding partner for newly synthesized CK1 δ . A PER2-dependent increase in CK1 δ 1 protein levels was also observed when HEK293T cells were transfected with a constant amount of CK1 δ 1 plasmid and increasing amounts of PER2 (Fig 4B). In contrast, coexpression of PER2 Δ CKBD, in which the CK1 binding domain (CKBD) is deleted, did not result in a substantial increase in CK1 δ 1 levels (Fig 4B). These findings indicate that the interaction between CK1 δ 1 and the CKBD of PER2 is critical for protecting the kinase from degradation. The modest stabilization of CK1 δ 1 observed with PER2 Δ CKBD may be due to the presence of an additional, albeit weak, CK1 δ 1 binding site within PER2 Δ CKBD⁵². Alternatively, this stabilization could occur indirectly through the PER2 Δ CKBD-dependent stabilization of endogenous PERs (see Fig 1C), which could then provide a binding site for CK1 δ 1.

To analyze whether CRY1 affects the stabilization of CK1 δ 1 by PER2, we expressed the proteins in HEK293T cells (Fig 4C). When PER2 was expressed alone, it remained hypophosphorylated. CRY1 alone was expressed at a low level. However, coexpression with PER2 led to an elevated expression of CRY1, consistent with the role of PER2 in protecting CRY1 from proteasomal degradation by occupying the FBXL3 binding site^{47,48}. Coexpression of CK1 δ 1 and CRY1 resulted in accumulation of low levels of both proteins. In contrast, when CK1 δ 1 was coexpressed with PER2, whether or not CRY1 was present, CK1 δ 1 accumulated at a high level. Since both CRY1 and CK1 δ 1 were tagged with a FLAG epitope, a comparison of their expression levels indicated that PER2 stabilized both proteins to a similar extent. Given that PER2 has a dedicated binding site for CRY1 and another for CK1 δ 1, this is consistent with a PER2 molecule stabilizing these proteins by binding a single molecule of each. The data suggest that, under conditions of overexpression, PER2 becomes saturated with CK1 δ 1 and CRY1. We observed that stabilized, i.e., PER2-bound CK1 δ 1 was capable of hyperphosphorylating PER2 while the kinase remained hypophosphorylated itself. Upon inhibition of phosphatases with Calyculin A (CalA), both PER2 and PER2-bound CK1 δ 1 underwent rapid hyperphosphorylation, indicating that PER2 does not inhibit the autophosphorylation of associated CK1 δ (Fig 4D). Instead, these findings suggest that cellular phosphatases act on both PER2 and PER2-bound CK1 δ , with a pronounced preference for dephosphorylating the kinase. Expression of PER2 and CRY1 in HEK293T cells also led to the accumulation of endogenous CK1 δ , consistent with the enrichment of CK1 δ in PER2-mNG:mK2-CRY1 nuclear foci observed in U2OStx cells (see Figure 2E). However, the concentration of endogenous CK1 δ remained well below the level required to saturate V5-PER2, indicating that its synthesis during the 24-hour timeframe of the experiment was insufficient to quantitatively bind all overexpressed PER2 molecules. Upon treatment with CalA, the entire population of overexpressed V5-PER2 became hyperphosphorylated, although to a lesser extent than under conditions of saturating CK1 δ 1. These findings suggest that PER2-anchored CK1 δ , present at substoichiometric levels, phosphorylated the excess V5-PER2 in a distributive manner rather than through a fixed, obligatory 1:1 stoichiometry. Accordingly, CK1 δ may dynamically equilibrate between individual PER2 molecules and/or act on multiple PER2 molecules within higher-order

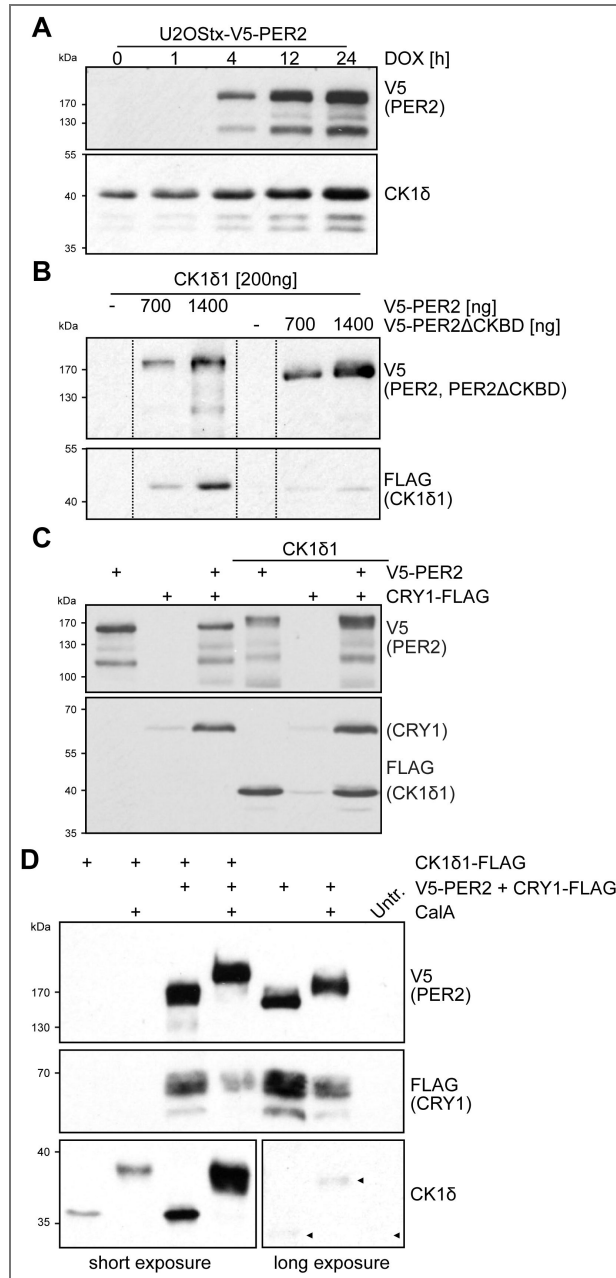


Fig 4. PER2 supports accumulation of endogenous CK1δ

(A) Endogenous CK1δ co-accumulates with overexpressed V5-PER2. Stable U2OSTx_V5-PER2 cells were DOX-induced and analyzed after the indicated time periods for expression of (upper panel) V5-PER2 and (lower panel) endogenous CK1δ. n = 3. (B) Overexpressed CK1δ is stabilized dependent on PER2 dosage and PER-CK1δ interaction. HEK293T co-expression of CK1δ1-FLAG (200 ng) with increasing V5-PER2 results in V5-PER2 dose-dependent stabilization of CK1δ1-FLAG. Coexpression with V5-PER2ΔCKBD does not substantially stabilize CK1δ1-FLAG. All samples are from the same gel and Western blot with the same exposure time. Dashed vertical lines indicate that gel lanes with lower PER2 levels and size marker lanes were spliced out. n = 3. (C) PER2 stabilizes CRY1 and CK1δ1. HEK293T cell expression of indicated combinations of V5-PER2, mK2-CRY1, and CK1δ1-FLAG. n = 3. (D) Phosphatase inhibition by CaIA promotes phosphorylation of PER2 as well as PER-bound CK1δ and affects levels of PER2-bound CRY1. HEK293T cell expression of indicated combinations of V5-PER2, CRY1-FLAG, and CK1δ1-FLAG with and without CaIA treatment. n = 3. Upper panel: CaIA promotes hyperphosphorylation of PER2. Middle panel: Levels of PER2-stabilized CRY1 correlate inversely with PER2 phosphorylation state. Lower panels: CaIA promotes phosphorylation of free CK1δ (lanes 1 and 2) as well as of PER2-bound (stabilized) overexpressed CK1δ (lanes 3 and 4) and PER2-bound endogenous CK1δ (lanes 5, 6 and 7). Note, the PER2-dependent stabilization of endogenous CK1δ by comparing with untransfected HEK293T cell control.

oligomeric assemblies. In the absence of CalA, however, the slow phosphorylation of V5-PER2 by substoichiometric levels of endogenous CK1 δ was efficiently counteracted by endogenous phosphatases.

To investigate whether the stabilization of CK1 δ 1 by V5-PER2 was affected by kinase activity, we expressed the catalytically inactive CK1 δ 1-K38R and tau-like mutant kinase, CK1 δ 1-R178Q³⁴. In the absence of V5-PER2, both mutant kinases were expressed at higher levels than CK1 δ 1, while CRY1 expression remained low (Fig EV4 [↗](#)). Coexpression with PER2 further stabilized both mutant kinases, resulting in their accumulation at levels slightly higher than CK1 δ 1 (comp. Figs 4C [↗](#) and EV4 [↗](#) from the same blot). The data suggest that V5-PER2 stabilizes active and mutant CK1 δ 1 at a 1:1 ratio, while any excess kinase is degraded in a manner correlated with its kinase activity.

Active kinase is primarily degraded in the nucleus

Active CK1 δ shuttles between the cytosol and the nucleus while kinase-dead CK1 δ -K38R accumulates in the nucleus⁵³. To further characterize the subcellular dynamics and how it relates with kinase activity and degradation, we analyzed the localization of CK1 δ , CK1 δ 1-R178Q and CK1 δ -K38R. Overexpressed CK1 δ 1 was highly enriched at the centrosome and displayed some enriched accumulation in the perinuclear region, as previously described^{54–56}, (Fig 5B [↗](#), left panels), similar to endogenous CK1 δ (Fig 5A [↗](#)). Kinase-dead CK1 δ 1-K38R accumulated in the nucleus, in agreement with a previous report⁵³. It was expressed at higher levels than CK1 δ 1, but did not localize to the centrosome (Fig 5B [↗](#), middle panels). Tau-like CK1 δ 1-R178Q, which is particularly compromised in its priming-dependent activity, was expressed at an intermediate level, somewhat enriched in the nucleus, and displayed centrosomal localization (Fig 5B [↗](#), right panels). These results suggest that the nuclear localization of CK1 δ 1 and its depletion from the centrosome is inversely related to its (priming-dependent) kinase activity. We confirmed this observation by treating U2OStx_CK1 δ 1 cells, and U2OStx cells for control, with either MG132 or PF670. Proteasomal inhibition with MG132 for 4 h led to an increase in overexpressed CK1 δ 1-FLAG throughout the cell and notably also at the centrosome (Fig 5C [↗](#)). The data demonstrate that centrosomal binding of CK1 δ was not saturated under untreated conditions, which may impact CK1 δ availability for other binding partners, such as PERs. CK1 δ 1 inhibited for 4 h with PF670 accumulated at elevated levels (Fig 5D [↗](#)). As reported previously⁵⁵ the kinase was depleted from centrosomes, and accumulated almost exclusively in the nucleus. These findings suggest that the inhibition of kinase activity affects turnover of overexpressed CK1 δ 1 as well as its accumulation in the nucleus and depletion from the cytosol and centrosome. Treatment of U2OStx control cells with MG132 or PF670 resulted in a small, non-significant increase in levels of endogenous CK1 δ (Fig EV5A, B [↗](#)). These data indicate that the physiological rate of kinase synthesis in U2OStx cells is rather low and insufficient to significantly increase CK1 δ expression above steady state levels within the 4 h treatment windows with MG132 and PF670.

To characterize CK1 δ 1 degradation independently of kinase activity we transiently transfected U2OStx cells with either CK1 δ 1-K38R-FLAG or CK1 δ 1-K38R-FLAG containing an N-terminal HIV-1 nuclear export signal (NES)⁵⁷. While CK1 δ 1-K38R localized to the nucleus and was depleted from the centrosome, NES-CK1 δ 1-K38R was found in the cytosol and the centrosome (Fig 5E [↗](#)). These results demonstrate that CK1 δ 1 facilitates nuclear export but not its localization to the centrosome per se. NES-CK1 δ 1-K38R was expressed at an ~5-fold higher level than CK1 δ 1-K38R (Fig 5E [↗](#)), suggesting that inactive kinase, despite its increased stability compared to CK1 δ 1, is preferentially degraded in the nucleus. Overall, the data indicate that unassembled active CK1 δ 1 is highly unstable and preferentially degraded in the nucleus (Fig EV5C [↗](#)). The enzymatic activity of CK1 δ 1 promotes both its nuclear export and the accelerated degradation of unassembled CK1 δ 1 in the nucleus, potentially through a shared mechanism such as activity-dependent release from nuclear binding sites.

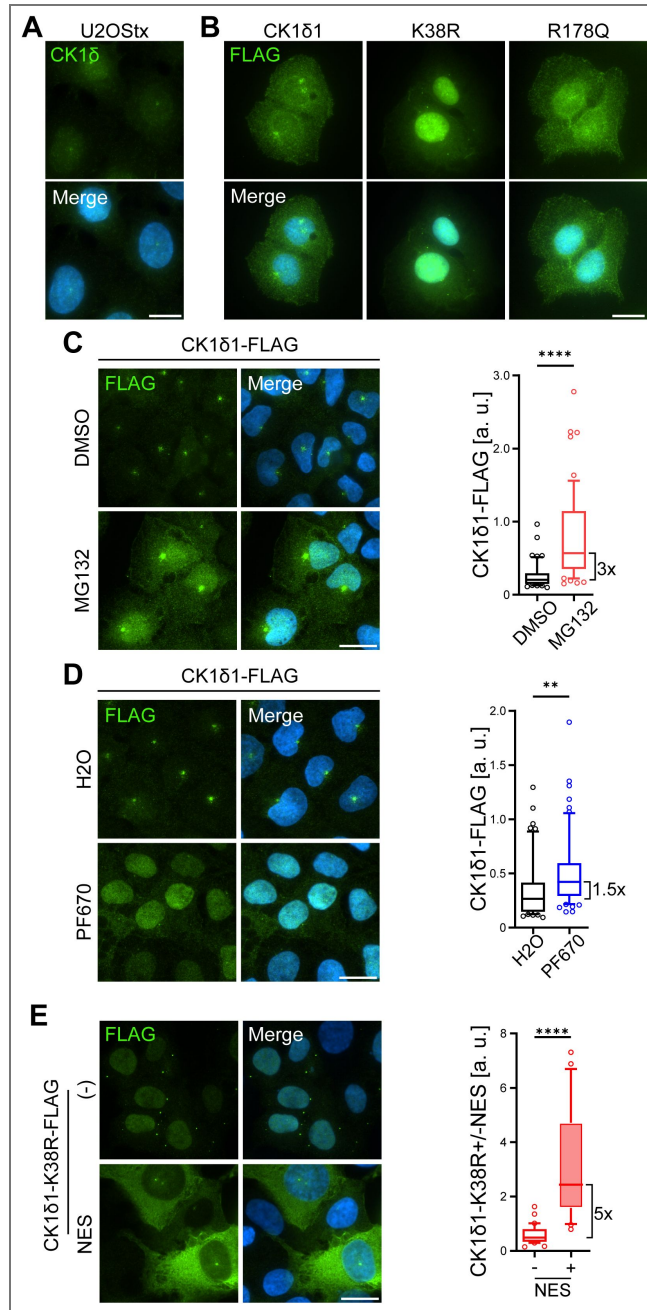


Fig 5. Active kinase is primarily degraded in the nucleus

(A) Endogenous CK1δ exhibits diffuse cellular localization with one distinct spot likely corresponding to the centrosome⁵⁵. U2OSx was stained with DAPI (blue) and an antibody against CK1δ (green; AF488). Scale bar 20 μm. (B) Immunofluorescence of U2OSx cell lines overexpressing FLAG-tagged CK1δ1, CK1δ1-K38R and CK1δ1-R178Q. Cells were DOX-treated for 24 h and stained via FLAG antibody (green; AF488) and with DAPI (blue). Scale bar 20 μm. n = 3. (C) Proteasomal inhibition by MG132 results in accumulation of overexpressed CK1δ1 primarily in nucleus. Stable U2OSx_CK1δ1 cells were DOX-induced for 24 h and treated with 5 μM MG132 for 4 h. Left: IF. Right: Quantification of CK1δ1 levels in MG132-treated cells versus vehicle (DMSO) control. n ≥ 50 cells; mean ± SD; ****: p < 0.0001. Scale bar 20 μm. (D) Kinase inhibition results in accumulation of overexpressed FLAG-tagged CK1δ specifically in the nucleus. Stable U2OSx_CK1δ cells were DOX induced for 24 h and treated with 1 μM PF670 for 1 h. Left: IF. Right: Quantification of CK1δ1 levels in PF670-treated cells versus vehicle (H₂O) control. n ≥ 50 cells; mean ± SD; **: p < 0.01. Scale bar 20 μm. (E) NES-tagged FLAG-CK1δ1-K38R accumulates at elevated levels in the cytoplasm and localizes to the centrosome. U2OSx cells were transiently transfected with either FLAG-CK1δ-K38R or NES-FLAG-CK1δ1-K38R. Left: FLAG-IF. Right: Quantification of kinase levels. n ≥ 20 cells; mean ± SD; ****: p < 0.0001. Scale bar 20 μm.

CK1 δ facilitates cytoplasmic accumulation of PER2 and release of CRY1

To analyze whether CK1 δ activity affects the localization and interaction of PER2 and CRY1, we transfected U2OStx_CK1 δ 1 and U2OStx_CK1 δ 1-K38R stable cells with PER2-mNG and mK2-CRY1. Expression and localization of the DOX-induced proteins was analyzed by live cell microscopy over a time course of 28 h. In U2OStx_CK1 δ 1-K38R, PER2-mNG alone accumulated initially in the cytosol and relocated slowly to the nucleus (Fig EV6A [↗](#), upper panels), similar to what was observed in absence of kinase (see Fig 1D [↗](#)). However, in U2OStx_CK1 δ 1 cells, PER2-mNG remained cytosolic (Fig EV6A [↗](#), lower panels). Considering that PER2-mNG shuttles rapidly between the nucleus and cytosol (see Fig 1A [↗](#)), the data suggest that co-expression of active CK1 δ 1 promotes cytoplasmic accumulation of PER2, potentially through inactivation of the NLS as shown for PER1³⁵. Upon expression of PER2 alone or coexpression of PER2-mNG and mK2-CRY1 in U2OStx_CK1 δ 1-K38R cells, PER2:CRY1 complexes accumulated in the nucleus and formed foci, which persisted for 28 h and longer (Fig EV6A [↗](#) and Fig 6A [↗](#), upper panels), similar to what was observed in absence of overexpressed kinase (see Fig 1D [↗](#), middle panels). The data indicate that the catalytically inactive CK1 δ 1-K38R did not affect the expression and localization of PER2-mNG and mK2-CRY1. Notably, PER2-mNG and mK2-CRY1 levels decreased in parallel over the 28-hour course of the experiment, with no free mK2-CRY1 remaining in the nucleus. In contrast, in U2OStx_CK1 δ 1 cells, PER2-mNG alone remained dispersed in the cytosol (Fig EV6A [↗](#), lower panels), while PER2-mNG and mK2-CRY1 accumulated in cytosolic foci with a substantial fraction of mK2-CRY1 accumulating in the nucleus independently of PER2-mNG (Fig 6A [↗](#), lower panels and EV6B). The foci grew in size up to about 12-16 h post DOX-induction. After approximately 20 hours, PER2-mNG was degraded, while mK2-CRY1 remained expressed and was exclusively detected in the nucleus. Nuclear mK2-CRY1 levels declined over time, but with substantially slower kinetics than those observed for cytoplasmic foci containing mK2-CRY1 and PER2-mNG. This suggests that free nuclear mK2-CRY1 represents a pool that either migrates to the nucleus upon phosphorylation-dependent PER2-mNG degradation and/or is released from PER2-mNG, potentially regulated by phosphorylation.

We then quantified the relative ratio of mK2-CRY1 to PER2-mNG in cytosolic versus nuclear foci. This analysis revealed that the cytoplasmic PER:CRY foci in cells expressing active CK1 δ 1 contained less mK2-CRY1 compared to the nuclear PER:CRY foci in cells expressing the inactive CK1 δ 1-K38R (Fig 6B [↗](#)), suggesting that a fraction of mK2-CRY1 is released from cytoplasmic foci prior to degradation of PER2-mNG. To investigate whether CK1 δ 1-mediated phosphorylation triggers the release of CRY1 from PER2 independently of phosphorylation-dependent PER2 degradation, we prepared a native cell extract from HEK293T cells overexpressing V5-PER2 and CRY1-FLAG which was then incubated with purified CK1 δ tail in an *in vitro* phosphorylation reaction³⁴. In the presence of kinase, PER2 was hyperphosphorylated while the electrophoretic mobility of CRY1 did not shift (Fig 6C [↗](#)). Subsequent immunoprecipitation revealed that CRY1 co-immunoprecipitated with unphosphorylated but not with hyperphosphorylated V5-PER2 (Fig 6C [↗](#)). The data suggest that CK1 δ 1-mediated phosphorylation of PER2 promotes the release of bound CRY1. Since free CRY is less stable, this result is consistent with the data shown above (Fig 4D, middle panel [↗](#)), where CalA-induced hyperphosphorylation of PER2 resulted in reduced CRY1 levels. To explore this further, we transfected stable U2OStx_mK2-CRY1 cells with PER2-mNG and untagged CK1 δ 1, and induced expression with DOX (Fig 6D [↗](#) and EV6C [↗](#)). The majority of cells expressed only mK2-CRY1, indicating that they remained untransfected. In contrast, cells exhibiting cytoplasmic foci of PER2-mNG were identified as cotransfected with untagged CK1 δ 1, as the foci become cytoplasmic only under these conditions. Tracking the DOX-induced protein dynamics over a 28-hour time course, we observed that mK2-CRY1 was depleted in untransfected cells, likely due to metabolism of DOX⁵⁸ and degradation of previously synthesized mK2-CRY1. Interestingly, in transfected cells, mK2-CRY1 initially colocalized with PER2-mNG in cytoplasmic foci. Upon PER2-mNG degradation, liberated mK2-CRY1 translocated and accumulated at elevated

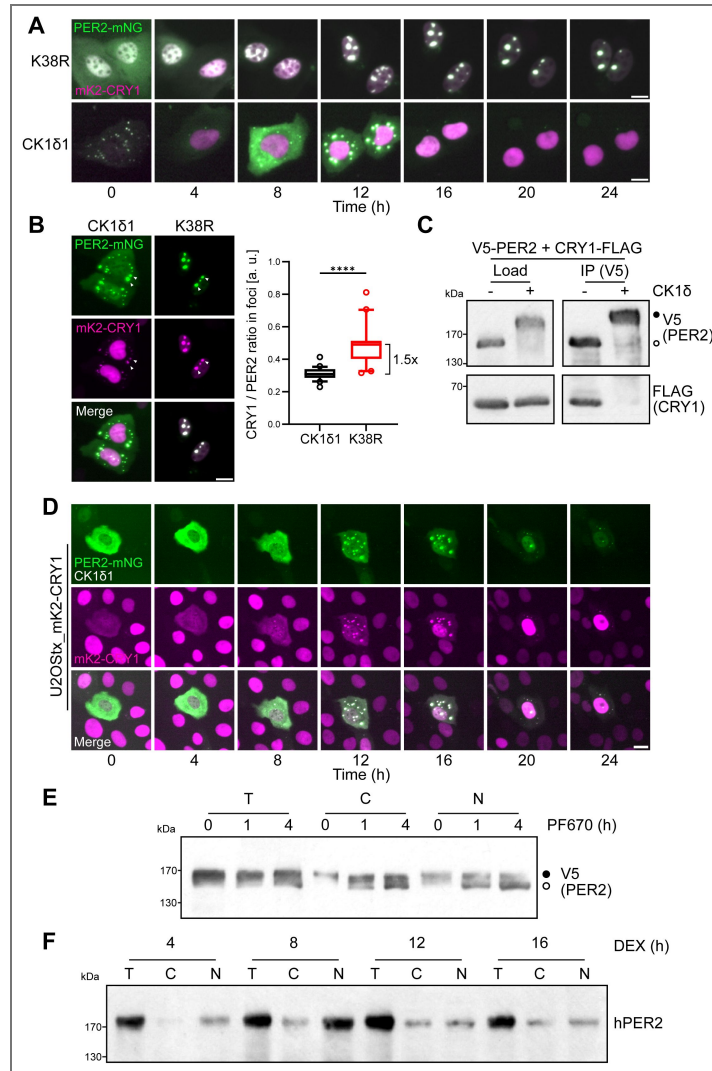


Fig 6. CK1δ facilitates cytoplasmic accumulation of PER2 and release of CRY1

(A) Transient transfection and coexpression of PER2-mNG and mK2-CRY1 in U2OStx_CK1δ1 and U2OStx_CK1δ1-K38R stable cell lines. Expression was DOX-induced 24 h post transfection and cells were then analyzed for 24 h with an Incucyte system. PER2-mNG and mK2-CRY1 accumulate in nuclear foci when coexpressed with inactive CK1δ1-K38R (upper row) and in cytoplasmic foci when coexpressed with active CK1δ1 (lower row). Scale bar 20 μm. (B) Cytoplasmic PER2-mNG foci (CK1δ1 cells) contain less mK2-CRY1 than nuclear foci (CK1δ1-K38R cells). Scale bar 20 μm. Right: Quantification of CRY1 : PER2 ratio in cytoplasmic and nuclear foci. n > 30 foci, mean ± SD; ****: p < 0.0001. (C) PER2 phosphorylation attenuates interaction with CRY1. V5-PER2 and CRY1-FLAG were transiently expressed in HEK293T. Cell lysate was prepared and incubated with and without recombinant CK1δtail for 4 h. V5-PER was then immunoprecipitated with V5 beads. Lysate (Input) and an 8x equivalent of the IP were analyzed by Western-blot. FLAG-CRY1 co-immunoprecipitated with hypophosphorylated but not with hyperphosphorylated V5-PER2. n = 3. (D) Cytoplasmic PER:CRY foci persistently release CRY1 into the nucleus in a CK1δ1-dependent fashion. Scale bar 20 μm. Central cell: Representative U2OStx_mK2-CRY1 cell co-transfected with PER2-mNG and CK1δ1, resulting in the formation of cytoplasmic PER:CRY foci. Over time, PER2-mNG levels decrease, while mK2-CRY1 accumulates in the nucleus and remains at persistently high levels, even 36 hours post DOX induction (see Fig EV6 for more examples). Surrounding cells: U2OStx_mK2-CRY1 cells not transfected with PER2-mNG. In these cells, mK2-CRY1 accumulates in the nucleus initially, but its levels decrease over time, likely due to DOX metabolism, with low levels observed 36 hours post DOX induction. (E) CK1δ inhibition by PF670 facilitated the nuclear accumulation of hypophosphorylated PER2. V5-tagged PER2 was transiently expressed in HEK293T cells together with FLAG-tagged CRY1 and CK1δ1. PF670 was added, and the subcellular localization of PER2 was analyzed at the indicated time points following PF670 treatment. (F) Endogenous PER2 subcellular redistribution from the nucleus to the cytosol in U2OStx cells was analyzed over a circadian cycle. U2OStx cells were synchronized with DEX at t = 0 h. After 4 and 8 h, endogenous PER2 was enriched in the nucleus. At later timepoints, a fraction of PER2 was localized in the cytosol.

levels in the nucleus. This led to sustained nuclear levels of mK2-CRY1 in cells initially expressing PER2-mNG and CK1 δ 1, even at later time points when mK2-CRY1 had already been depleted in neighbouring untransfected U2OStx_mK2-CRY1 cells.

To investigate the impact of phosphorylation on PER2 subcellular localization, we co-expressed V5-PER2, FLAG-CRY1, and FLAG-CK1 δ in HEK293T cells. The cells were then treated with the CK1 inhibitor PF670, and the subcellular localization of PER2 was analyzed. Before PF670 treatment, PER2 was hyperphosphorylated and predominantly localized in the cytosol. Treatment with PF670 for 1 and 4 hours led to dephosphorylation indicating that PER2 phosphorylation was antagonized by phosphatases. This dephosphorylation facilitated nuclear accumulation of a substantial fraction of PER2 (Fig 6E [↗](#)). Finally, to assess the impact of PER2 phosphorylation on its subcellular localization within the context of a functional circadian clock, PER2 localization was monitored over a circadian cycle in dexamethasone (DEX)-synchronized U2OS cells (Fig 6F [↗](#) and EV6D [↗](#)). At early time points after synchronization, PER2 was predominantly localized in the nucleus but partially redistributed to the cytosol at later time points, consistent with previous microscopy and immunoblot analyses of the subcellular distribution of endogenously tagged PER2^{15,43,59}.

Cytoplasmic localization of PER2 and CRY1 has also been reported under physiological conditions in the SCN¹⁸. Consistent with our observations, the CRY1-to-PER2 ratio in SCN neurons was significantly lower in the cytosol than in the nucleus. It has previously been shown that nuclear CRY1 forms a repressive complex with CLOCK:BMAL1 late in the circadian cycle^{11,15}. Our data suggest that cytoplasmic PER2, and the resulting cytoplasmic PER2:CRY1 complexes, may function as a reservoir that gradually releases CRY1 into the nucleus in a CK1 δ 1-dependent manner, a process formally analogous to the de novo synthesis of CRY1 from its mRNA. In this model, phosphorylation-dependent cytoplasmic retention of PER2 and the slow release of CRY1 would serve to decouple CRY1's subcellular localization, repressive activity, and degradation from those of PER2.

Nuclear CK1 δ 1 affects circadian period length

Our data show that overexpressed and unassembled CK1 δ 1 in the nucleus is rapidly degraded or exported. To analyze how nuclear and cytosolic CK1 δ 1 affect the circadian clock, we constructed V5-CK1 δ 1 fusion proteins with an N-terminal mNeonGreen tag followed by either an SV40 nuclear localization signal (NLS)⁶⁰ or an HIV-1 nuclear export signal (NES)⁵⁷ (Fig 7A [↗](#)). To characterize the subcellular localization and stability of the kinases, U2OStx cells were transiently transfected with these mNG-CK1 δ 1 constructs. Next day, the expression was induced with DOX for 24 h, and cells were then treated with or without MG132 for 4 h. mNG-NLS-CK1 δ 1 was expressed at a low level and localized to the nucleus (Fig 7b [↗](#), left panel), while mNG-NES-CK1 δ 1 accumulated in the cytosol (Fig 7b [↗](#), right panel), demonstrating that the added localization signals determined the subcellular distribution of the shuttling kinases. MG132 treatment stabilized mNG-NLS-CK1 δ 1 about 8-fold (Fig 7B [↗](#)), while mNG-NES-CK1 δ 1 was stabilized only about 1.8-fold (Fig 7C [↗](#)). The data indicate that, in the absence of MG132, overexpressed mNG-NLS-CK1 δ 1 is rapidly degraded by the nuclear proteasome, while overexpressed mNG-NES-CK1 δ 1 is turned over at a lower rate because it escapes efficient nuclear degradation by enhanced export into the cytosol. We then generated and selected stable U2OStx cell lines expressing in DOX-inducible manner similar levels of mNG-NLS-CK1 δ 1 and mNG-NES-CK1 δ 1, respectively (Fig 7D [↗](#)). To monitor the circadian rhythm, cells were transfected with a *Bmal1* promoter (*Bmal1p*-*luc* reporter). Cells were then incubated with or without DOX and *Bmal1p*-*luc* expression was recorded for 96 h. Expression of mNG-NLS-CK1 δ 1 shortened the circadian period by 4 h (Fig 7E [↗](#), upper panel and F), while mNG-NES-CK1 δ 1 had no impact on period length (Fig 7E [↗](#), lower panel and F). The data demonstrate that cytoplasmic mNG-NES-CK1 δ 1 does not interfere with the function of endogenous PER proteins, indicating that CK1 δ is not functionally limiting in the cytosol. Because period length is determined by nuclear CK1 δ activity, these findings further imply that the nuclear CK1 δ pool is insufficient to fully saturate PER proteins, regardless of where newly synthesized PERs initially acquire the kinase (Fig. EV7 [↗](#)).

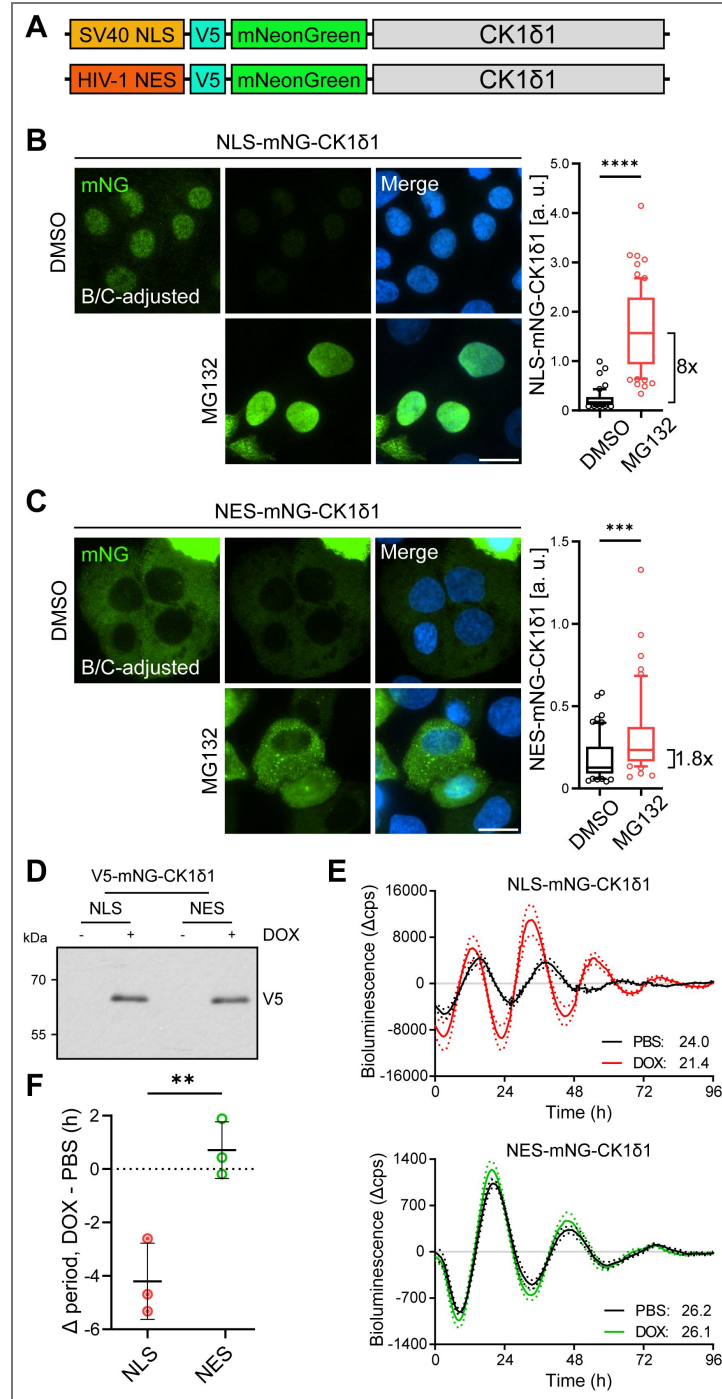


Fig 7. Nuclear CK1δ affects circadian period length

(A) Schematic of mNG-V5-NLS-CK1δ and mNG-V5-NES-CK1δ constructs NLS: SV40⁵⁷; NES: HIV-1¹⁶⁰. (B) Left: mNG-NLS-CK1δ is expressed at a very low level in the nucleus and is stabilized by MG132. B/C-adjusted: brightness and contrast adjusted to better visualize the kinase. Right: quantification. n > 30 cells, mean ± SD; ****: p < 0.0001. Scale bar 20 μm. (C) Left: mNG-NES-CK1δ localizes to the cytosol and is stabilized by MG132. Right: quantification. n > 30 cells, mean ± SD; ***: p < 0.001. Scale bar 20 μm. (D) Stable U2OSx lines expressing comparable levels of DOX-induced V5-tagged mNG-NLS-CK1δ or mNG-NES-CK1δ. n = 3. (E) DOX-induced expression of NLS-CK1δ results in significant period shortening whereas NES-CK1δ has no effect on period. *Bmal1* promoter-luciferase assay. Representative bioluminescence traces are shown as a detrended average of 4 technical replicates of PBS- and DOX-treated cells. Resulting period was calculated using cosinor analysis built-in GraphPad Prism 10. n = 3. (F) Circadian period change comparing DOX- vs. PBS-treated mNG-NLS-CK1δ or mNG-NES-CK1δ cell lines. n = 3, mean ± SD; **: p < 0.01.

Discussion

The current dual-mode circadian repression model describes three distinct phases of CLOCK:BMAL1 activity, regulated in temporal succession by CRY1/2, PER1/2, and CK1 δ ^{13–17,59}. Initially, CLOCK:BMAL1 is predominantly repressed via PER:CRY:CK1 δ -mediated displacement from its target genes, followed later by CRY1-dependent blocking of DNA-bound CLOCK:BMAL1, and finally derepression of CLOCK:BMAL1 when PER proteins are degraded and CRY1 levels decline below a critical threshold. Within the framework of current circadian clock models, CK1 δ is assumed to be non-limiting and readily available to PER proteins as they are synthesized in the cytosol, thereby ensuring robust and precise timekeeping.

The data presented here suggest that freely available CK1 δ is limited within the nucleus. Previous work has shown that nuclear export of CK1 δ depends on its kinase activity⁵³. We confirm these findings and extend them by demonstrating that unassembled nuclear CK1 δ is subject to rapid degradation, with turnover further accelerated by its catalytic activity. Mechanistically, the activity dependence of both processes may reflect a shared mechanism, such as activity-dependent release from nuclear binding sites. Moreover, we show that CK1 δ is stabilized through association with PER2. The data align with earlier findings and provide a mechanistic explanation for why nuclear CK1 δ levels in mouse liver remain very low in the absence of PER proteins, but increase in parallel with the circadian accumulation of nuclear PER, while cytoplasmic CK1 δ levels remain constant and higher than those in the nucleus⁵⁹. Complex formation between CK1 δ and PER proteins is well established as essential for circadian timekeeping¹¹, with CK1 δ 1 overexpression known to shorten circadian period length³⁴. Our results suggest that the subcellular distribution of CK1 δ is finely tuned and suggest that nuclear concentrations remain below the threshold required for PER saturation. Specifically, overexpression of NLS-tagged CK1 δ shortens period length, whereas NES-tagged CK1 δ has no detectable effect. This is consistent with previous studies showing that PER associates with CK1 δ in the cytosol and enters the nucleus facilitated by CRY^{3,15,59}. Because each PER molecule can import only one kinase, a process that likely occurs at wild-type levels of cytosolic CK1 δ , overexpression of NES-tagged CK1 δ does not increase the nuclear CK1 δ pool. When the few CK1 δ molecules co-imported with PER:CRY complexes equilibrate with the unbound nuclear pool, rebinding to PER is constrained by rapid degradation of nuclear CK1 δ or its export to the cytosol. In contrast, NLS-tagged CK1 δ overexpression directly increases nuclear kinase abundance by antagonizing nuclear degradation as well as export.

Thus, when evaluating the impact of CK1 δ / ϵ mutants on the circadian clock, not only kinase activity but also protein stability and subcellular distribution must be taken into account. Indeed, we observed that the altered activity of the tau-like CK1 δ 1-R178Q mutant affects its subcellular localization and turnover, leading to its accumulation at elevated levels in the nucleus. Analysis of the PER2 phosphoswitch provides strong evidence that the tau mutation (e.g., R178C in CK1 δ) shortens the circadian period by attenuating phosphorylation of the FASP region in PER2 while accelerating phosphorylation of the β -TrCP degron site (S478 in mPER2)^{30–32}. We demonstrate that the period shortening induced by the tau-like CK1 δ 1-R178Q mutant³⁴ can be partially replicated by forcing nuclear accumulation of wild-type CK1 δ 1 using an NLS tag (mNG-NLS-CK1 δ 1). Thus, the elevated nuclear accumulation of tau-like kinase may, in addition to its altered substrate specificity^{32,61}, contribute to the period-shortening phenotype observed in tau mutant animals^{62,63}.

This study examines the subcellular localization and interplay between PER:CRY:CK1 δ complexes and CRY1. In the prevailing circadian model, transcriptional feedback is driven initially by the nuclear accumulation of PER:CRY:CK1 δ repressor complexes. This is followed in the late phase by sustained repression mediated by CRY1 alone, which persists for several hours after CK1 δ -dependent degradation of PER proteins. However, evidence from mouse liver⁵⁹, SCN slices¹⁸, and U2OS cells⁴³ and this study indicates that a substantial fraction of PER2 remains cytoplasmic, even when CRY1 is present, which normally supports nuclear import of the PER:CRY complex. While several mechanisms underlying cytoplasmic localization of PER2 have been proposed^{38,64}, no circadian function has yet been attributed to the cytosolic PER2 pool.

We show by transient transfection and overexpression that the distribution of PER2 between cytoplasm and nucleus depends on the expression ratio of PER2 and CRY1. DOX-induced transient overexpression was necessary to analyze how PER2 and CRY1 influence each other's subcellular localization and dynamics while excluding contributions from endogenous PER1 and CRY2. Our data suggest that PER2 dimers and dimers bound by a single CRY1 molecule are predominantly cytosolic, whereas dimers bound by two CRY1 molecules are enriched in the nucleus (see Fig 1E). In the physiological context of a functional clock, PER1, CRY2, PER2, and CRY1 are rhythmically expressed with consecutive peaks at different CTs^{12,65}. Since their expression ratios and levels vary over the course of a circadian cycle⁶⁵, the composition and saturation of PER complexes by CRYs depend on both their specific expression levels, subcellular localization and binding affinities. Furthermore, our data show that CK1 δ -mediated phosphorylation promotes dissociation of bound CRY1, thereby supporting the cytoplasmic accumulation of PER2 dimers containing one or no CRY1 molecule. In the context of a functional circadian clock in U2OS cells, we observe that the subcellular distribution of PER2 shifts from predominantly nuclear to increasingly cytoplasmic over the course of the circadian cycle, consistent with our overexpression data. Inhibition of CK1 δ/ϵ reverses this process, leading to dephosphorylation of cytosolic PER2 and its accumulation in the nucleus. Consistent with these observations, hyperphosphorylated PER2 is predominantly cytoplasmic in mouse liver⁵⁹ and U2OS cells⁴³.

Incorporating these findings into the current circadian framework, we propose that the transition between the early and late repressive phases involves a decline in nuclear PER2:CRY1:CK1 δ complex levels, driven by both PER2 degradation and cytoplasmic relocalization. PER2 degradation and reduction of nuclear PER2:CRY1:CK1 δ complexes by export below a critical threshold could provide a time window for CLOCK dephosphorylation and facilitate subsequent rebinding of CLOCK:BMAL1 to DNA. In addition, cytoplasmic PER2:CRY1:CK1 δ complexes could act as a reservoir, gradually releasing CRY1 in a CK1 δ -dependent manner to support repression of DNA-bound CLOCK:BMAL1, complementing *de novo* CRY1 synthesis, which peaks as PER2 levels fall. The contribution to repression by newly synthesized CRY1 and by CRY1 released from cytosolic PER2 could vary by cell type and physiological conditions. Supporting this, our data show that nuclear CRY1 levels are markedly higher and more sustained in CRY1-expressing U2OS cells that overexpress and accumulate PER2 and CK1 δ in the cytosol.

The fact that both PER1/2:CRY1/2:CK1 δ complexes and CRY1 alone repress CLOCK:BMAL1 raises the question of whether the mammalian circadian clock gains a functional advantage from maintaining both repressive modes. Published data indicate that CRY1 is present and functionally active throughout the entire circadian cycle^{18,66}. Although both PER and CRY proteins are rhythmically expressed, quantitative analyses reveal that PER protein levels are very low when CLOCK:BMAL1 activity reaches its circadian maximum, whereas CRY1 remains at ~50% of its peak level^{18,65}. Moreover, ChIP-seq analyses in mouse liver show that CRY1 is bound to circadian promoters not only during the late repressive phase (CT0-4), but also at CT8-12, when CLOCK:BMAL1 activity is maximal¹². Finally, studies of endogenously tagged PER2-LUC demonstrated that PER2 oscillates around an elevated baseline in CRY1 knock-out U2OS cells and around a reduced baseline in CRY2 knock-out cells⁶⁶. These findings suggest that in U2OS cells, CRY1 partially represses CLOCK:BMAL1 even during the circadian peak of transcription. Together, these observations support the view that CRY1 attenuates CLOCK:BMAL1 activity across the entire circadian cycle. Consequently, whereas PER1/2:CRY1/2:CK1 δ complexes primarily regulate the troughs of circadian gene expression, CRY1 may act to limit the peak amplitude of CLOCK:BMAL1-dependent transcription, thereby enhancing the dynamic range and responsiveness of the clock during this phase.

In summary, our data suggest that cytoplasmic CK1 δ is readily available to assemble in a one-to-one complex with PER proteins. After nuclear import of the PER:CRY:CK1 δ complex, the bound kinase will equilibrate with the nuclear CK1 δ pool. Because the nuclear CK1 δ concentration is low, rebinding of CK1 δ may not allow saturation of PERs in steady state. This provides a mechanistic explanation for why overexpression of nuclear CK1 δ shortens circadian period length while overexpression of cytosolic CK1 δ has no effect. Moreover, our overexpression data suggest that

CK1 δ -mediated phosphorylation disrupts PER2-CRY1 complexes, promoting the buildup of cytosolic PER2 complexes with substoichiometric CRY1 bound, while unbound CRY1 may gradually accumulate in the nucleus, a process analogous to nuclear import of newly synthesized CRY1. In the physiological context of a functional clock, the redistribution of CRY1 could contribute to establishing the poised promoter state with CLOCK:BMAL1.

Many of our conclusions are derived from, synchronized DOX-induced overexpression of tagged clock proteins combined with time-lapse live-cell microscopy. While this approach was necessary to capture mechanistic insights that would be technically challenging or impossible to resolve under physiological protein levels, it will require further validation with other methods and in other systems. Nonetheless, our findings align well with and recontextualize independent observations of clock protein levels, phosphorylation states, and subcellular localization in mouse liver^{11,59} and the SCN^{18,46}, thereby contributing to our understanding of the repressive phase of the core circadian clock.

Methods

Plasmids

For cloning using restriction enzymes. Enzymes used for cloning were obtained from New England Biolabs (NEB). Restriction digestion, dephosphorylation of vector backbone and ligation was performed as recommended by NEB. Linear DNA was purified using NucleoSpin Gel and PCR Clean-up kit from Macherey-Nagel. Plasmids were extracted with GeneJET Plasmid Miniprep kit from Thermo Fisher Scientific. For cloning with overlapping regions (restriction enzyme-free cloning), enzymes (Q5 DNA polymerase, restriction enzyme DpnI and T4 DNA polymerase) were obtained from NEB. DpnI digestion and exonuclease reaction with T4 DNA polymerase was performed in NEBuffer 2.1. *E. coli* were transformed with exonuclease treated PCR product(s) to facilitate *in vivo* plasmid assembly via overlapping DNA ends. pcDNA4/TO-derived vectors were constructed by cloning the coding regions of human casein kinase 1 isoform delta (CK1 δ), murine Period circadian protein homolog 2 (mPer2), and murine cryptochrome 1 (mCry1) downstream of the CMV-TetO2 promoter which allows for DOX-inducible protein expression in cells harboring the tetracycline-repressor cassette (tx; i.e., U2OStx) and constitutively high expression in cells without the tetracycline-repressor cassette (i.e., HEK293T). Mutations, fluorescent tags, and epitopes were introduced by via ligation-free overlap cloning. All plasmid DNA sequences were sequence-verified prior to use.

Cell lines

T-REx-U2OS (U2OStx; Life Technologies) and HEK293T (ATCC) cells were maintained in Dulbecco's Modified Eagle Medium (DMEM) supplemented with 10% Fetal Bovine Serum (FBS) and 1x Penicillin-Streptomycin (Pen-strep). Cell culture reagents were obtained from Life Technologies. Cells were grown and maintained at 37°C in a humidified incubator containing 5% CO₂.

For plasmid transfection, U2OStx cells were transfected with Xfect Transfection Reagent (Takara) following the manufacturer's protocol whereas HEK293T cells were transfected with polyethylenimine (PEI, made in-house) following the conventional protocol. To generate stable U2OStx cell lines, basal U2OStx cells were seeded in a 24-well plate and grown to confluence overnight. Cells were transfected with pcDNA4/TO vectors containing the desired constructs. Stable transfectants were selected by growing cells to sub-confluence in complete media supplemented with 50 μ g/mL hygromycin and 100 μ g/mL zeocin (Invitrogen) over the course of two to three weeks. Resulting single cell colonies after selection were isolated for further experimentation as previously described. To induce protein overexpression, cells were treated with 10 ng/mL DOX.

Immunofluorescence

Cells were seeded on 12mm #1.0 glass coverslips (VWR, CAT# 631-1577P) in 500 μ L media. Whenever applicable, transient transfection and/or DOX induction was performed. Immunofluorescence was done 24 h post-induction. Cells were washed with PBS and fixed with 4% paraformaldehyde for 10 min at room temperature. Cells were permeabilized with PBS + 0.1% Triton X-100 for 10 min, then washed three times and blocked with PBS + 5% heat-inactivated FBS for 1 h. Cells were then treated with the following primary antibodies diluted in PBS + 3% BSA + 0.25% Tween20 for 1 h at 37°C: PER2 (in-house, 1:50, rabbit polyclonal), PER1 (in-house, 1:100, rabbit polyclonal), BMAL1 (in-house, 1:200, rabbit polyclonal)^{67,68}, CK1 δ (Abcam ab85320, 1:1000), FLAG (Sigma-Aldrich F3165, 1:200). This was followed by washing with PBS, and treatment with corresponding secondary antibody: goat anti-rabbit conjugated to AlexaFluor488 (Thermo Fisher Scientific A-11008, 1:500) or goat anti-mouse conjugated to AlexaFluor488 (Thermo Fisher Scientific A-11001, 1:500) diluted in PBS + 3% BSA + 0.25% Tween20 for 1 h at 37°C. Cells were again washed three times, then mounted onto glass slides with ProLong™ Glass Antifade Mountant with NucBlue (Thermo Fisher Scientific P36983) and sealed with nail polish.

Fluorescence, time-lapse, and live-cell confocal microscopy

For microscopy of fluorescently-tagged proteins and immunofluorescence, a Nikon Ni-E microscope was used (Nikon Imaging Center, Heidelberg) at a 60X oil immersion objective and the corresponding filter sets for DAPI, FITC, and Cy5. Exposure times were optimized within each experiment to obtain comparable fluorescence intensities. For image acquisition, the central focal plane was determined and images were taken as at 0.3 μ m z-steps to a total 11 steps. For time-lapse microscopy, an Incucyte S3 system (Sartorius) was used at a 20X objective using the built-in filter sets set for the green and red channel. Exposure times were optimized within each experiment to obtain comparable fluorescence intensities. Images were taken at a regular schedule every 4 h until the end of the experiment typically 48 h later. For time-lapse, live-cell, confocal microscopy, a Nikon A1R confocal microscope was used (Nikon Imaging Center, Heidelberg) with a built-in TokaiHit on-stage environmental chamber. To prevent autofluorescence, colorless DMEM supplemented with normocin was used. Additionally, 60X oil immersion objective and the corresponding laser and filter sets for DAPI, FITC, TRITC, and TD (brightfield) were used. Exposure times were optimized within each experiment to obtain comparable fluorescence intensities. For image acquisition, the central focal plane was determined and images were taken as at 1.5 μ m z-steps to a total 5 steps. Images were taken every 5 min for 17 h. All resulting images were exported and digital image analysis was performed in FIJI.

Quantitative PCR

Cells were grown in p24 plates and induced with DOX for 24 h. RNA was extracted using peqGOLD TriFast Reagent following manufacturer's protocols. cDNA was reverse-transcribed from 500 ng total RNA extract with Maxima Reverse Transcriptase (Thermo Fisher Scientific) following manufacturer's protocols. Quantitative PCR (qPCR) was performed on a StepOne™ Real-Time PCR System (Applied Biosystems, Thermo Fisher Scientific, CAT# 4376598) using Maxima SYBR Green qPCR Master Mix (Thermo Fisher Scientific) following manufacturer's protocols. The following primer pairs below were used for their respective targets: CK1-F: AACCAAACACCCTCAGCTCCAC and CK1-R: GCCCAGCAGCTCCATACCCAT; GAPDH-F: TGCACCACCAACTGCTTAGC and GAPDH-R: ACAGTCTTCTGGGTGGCAGTG. Relative gene expression was normalized to GAPDH and calculated using the $\Delta\Delta C_T$ method. Further normalization to the DOX-induced U2OStx sample was done to determine fold induction of gene expression.

Immunoblotting

Protein extraction was performed using an in-house lysis buffer (25 mM Tris-HCl, pH 8.0, 150 mM NaCl, 0.5% Triton X100, 2 mM EDTA, 1 mM NaF, freshly added protease inhibitors: 1 mM phenylmethylsulfonyl fluoride (PMSF), leupeptin (5 μ g/ml), and pepstatin A (5 μ g/ml)) according to the conventional protocol. Briefly, cells were scraped and sample was collected via centrifugation.

The sample was incubated in ice-cold lysis buffer on ice for 10 min and then incubated in a sonicated water bath for 10 min. Samples were centrifuged at 16,000 x g, 4 °C, 15 min taking the supernatant. Protein concentration was quantified via Nanodrop (NP80, Implen). For immunoblot analysis, protein samples were analyzed by SDS-polyacrylamide gel electrophoresis and transferred to a nitrocellulose membrane (cytiva, Amersham Protran, 0.45 µm pore size) via semi-dry blotting. To control for protein loading, membranes were stained with Ponceau S. Membranes were typically incubated in primary antibody at 4°C overnight and in secondary antibody conjugated to horseradish peroxidase at room temperature for 2 h. The following primary antibodies were used: anti-FLAG (Sigma-Aldrich F3165, 1:5000, mouse monoclonal), anti-CK1δ (abcam AF12G4, 1:5000, mouse monoclonal), anti-V5 (Invitrogen R960-25, 1:5000, mouse monoclonal); and the following secondary antibody was used for luminescent detection: goat anti-mouse IgG (H+L)-HRP conjugate (Bio-Rad 170-6516, 1:10000). For decoration, membranes were incubated in decoration buffer (100 mM TrisHCl pH 8.5, 2.2 x 10⁻² % (w/v) luminol, 3.3 x 10⁻³ % (w/v) coumaric acid, 9.0 x 10⁻³ % (v/v) H₂O₂) and exposed for a time series to X-ray films (Fujifilm). Films were then developed (Medical film processor from Konica Minolta). Densitometric analysis of immunoblots was done using the built-in module in FIJI. The results were measured and plotted onto GraphPad Prism for downstream analysis (i.e., plotting over time post-CHX chase).

LMB treatment; CHX chase; MG132, PF670, CalA treatments

Unless otherwise stated, induction of protein expression was typically performed by addition of 10 ng/mL doxycycline (DOX; Thermo Fisher Scientific CAT# 631311) 24 h prior to downstream experiments. To inhibit CRM1-dependent nuclear export, LMB was added to cells to a final concentration of 20 nM; an equivalent volume of methanol was added to cells as a negative control. To arrest protein translation for a cycloheximide (CHX) chase, CHX was added to cells to a final concentration of 10 µg/ml. Untreated samples were taken as the 0 min CHX sample. Samples were then taken at 15, 30, 45, 60, and 90 min post-CHX for protein extraction and immunoblotting. To inhibit the proteasome, cells were treated with 20 µM MG132 (Abmole Bioscience CAT# AMO-M1902) for 4 h prior to immunoblotting; 4 µM MG132 for 4 h prior to immunofluorescence. To inhibit CK1δ; cells were treated with 1 µM PF670462 (Tocris Biosciences CAT# 3316) for 4 h prior to immunoblotting and immunofluorescence. To inhibit phosphatases, cells were treated with 80 nM CalA (LC Labs Cat# C-3987) for 1 h. All chemical treatments were performed with the corresponding solvent (vehicle) control: DMSO for MG132 and CalA, and H₂O for PF670.

In vitro phosphorylation assay and co-immunoprecipitation

HEK293T cells were transfected with V5-PER2 and CRY1-FLAG and the lysate was used as a starting material for an *in vitro* phosphorylation assay. CK1δ Δ tail was purified and used as the kinase for an *in vitro* phosphorylation assay as previously described³⁴. As a negative control, a reaction mix containing all of the reaction buffer components except for the MgCl₂ was incubated with the sample in the absence of additional kinase. The *in vitro* phosphorylation reaction was carried out at 4°C for 6 h. The reaction was stopped using PF670 prior to subsequent co-IP. For co-IP, Protein G Sepharose 4 Fast Flow (cytiva, 17061802) beads were used following the manufacturer's protocol. Briefly, a 1:1 slurry was prepared by repetitive washing and buffer exchange with 67% TBS. The beads were then incubated with anti-V5 antibody (Thermo Fisher Scientific, R960) at 4°C while rotating for 4 h and used directly. Resulting samples following an *in vitro* phosphorylation assay were loaded onto the beads and incubated at 4°C overnight. Supernatant was removed, and the beads were then washed thrice with cold 67% TBS and gently centrifuged at 300 x g, 4°C, for 30 s. Bound protein was eluted using 2x Laemmli buffer without β -mercaptoethanol and boiling at 95°C for 5 min. Corresponding "Input" and "IP" samples were taken and loaded onto a PAGE gel. For the IP sample, an 8x equivalent was loaded compared to Input.

Dexamethasone treatment and synchronization

As an additional synchronization cue aside from media change, U2OStx cells were synchronized using dexamethasone (DEX, dissolved in ethanol) at a working concentration of 1 μ M. At the designated timepoints, cells were treated with DEX for 20 min, followed by washing with 1x PBS. The medium was then replaced with fresh D10 marking the start of the time post-DEX synchronization. Cells were then harvested at 4, 8, 12, and 16 h post-DEX synchronization.

Subcellular fractionation

To separate the cytosolic and nuclear cellular fractions, the NE-PER™ Nuclear and Cytoplasmic Extraction Kit (Thermo Fisher Scientific, Cat #78833) was used following the manufacturer's instructions.

Luciferase reporter assay

Bioluminescence of luciferase reporter genes was performed as previously described³⁴. Briefly, samples were measured with a plate reader (EnSpire from PerkinElmer) placed in a temperature-controlled incubator (CLF Plant Climatics E41L1C8). Cells were seeded in a white 96-well plate and transfected using Xfect with *Bmal1p*-luc vector⁶⁹. Cells were synchronized via medium change using media supplemented with either PBS or DOX. The plate was sealed and bioluminescence was recorded at 30 min intervals at 37°C. Three independent experiments with four technical replicates per cell line and treatment were carried out. Resulting bioluminescence traces were detrended using a sliding 24h-time window for baseline subtraction and a sliding 3h-time window for smoothing. Circadian period was determined using the curve-fitting function to a non-linear damped sine wave function in GraphPad Prism 10.

Statistical Analysis

Data were plotted on GraphPad Prism 10. To test for differences between two samples, student's t-test was performed. To test for difference between three or more samples, ANOVA was performed. Statistical significance was defined by a p value of < 0.05. All data are presented as means \pm standard deviations (SD).

Supplementary figures

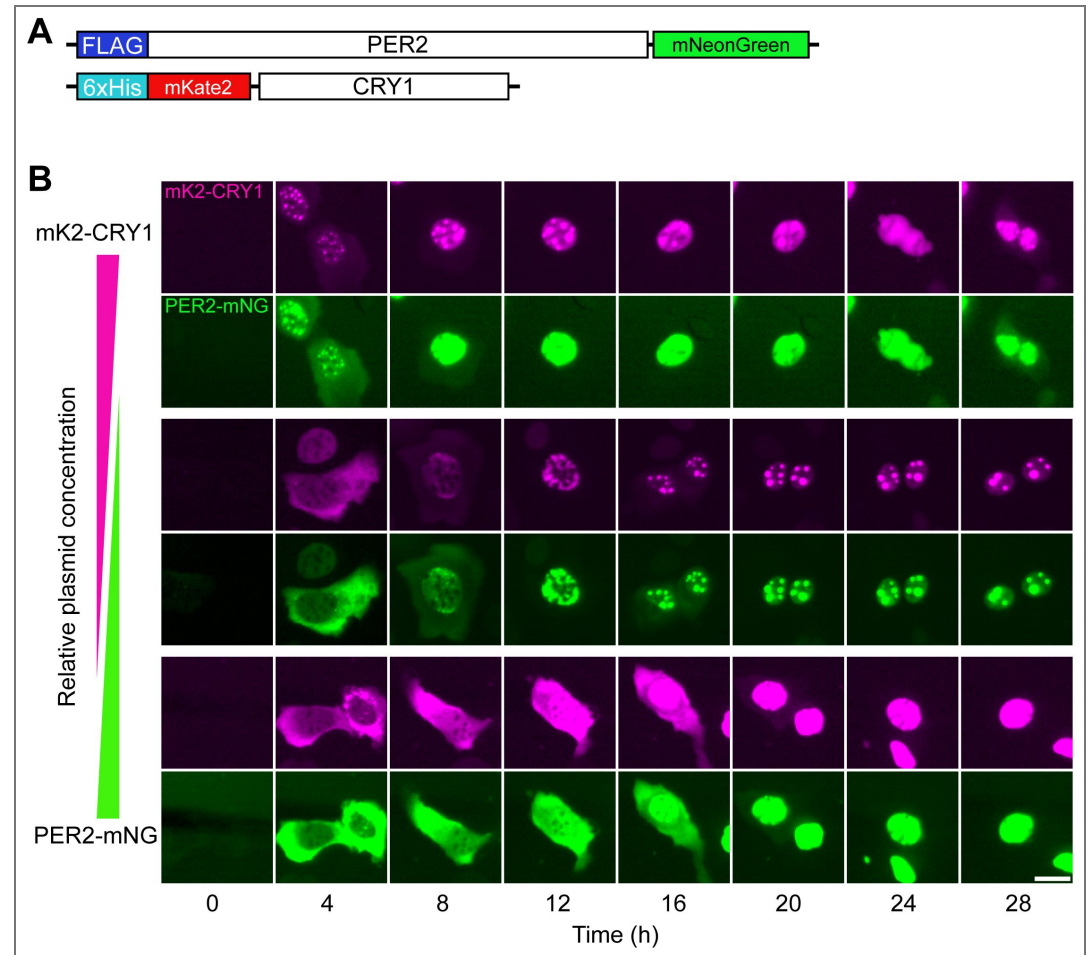


Fig EV1. Subcellular dynamics of overexpressed PER2 and CRY1. (A) Constructs used in this study: FLAG-PER2-mNeonGreen (PER2-mNG) and 6xHis-mKate2-CRY1 (mK2-CRY1). (B) Individual channels from the middle rows of Fig 1C, showing the localization of mK2-CRY1 (magenta) and PER2-mNG (green), respectively. Scale bar: 20 μ m.

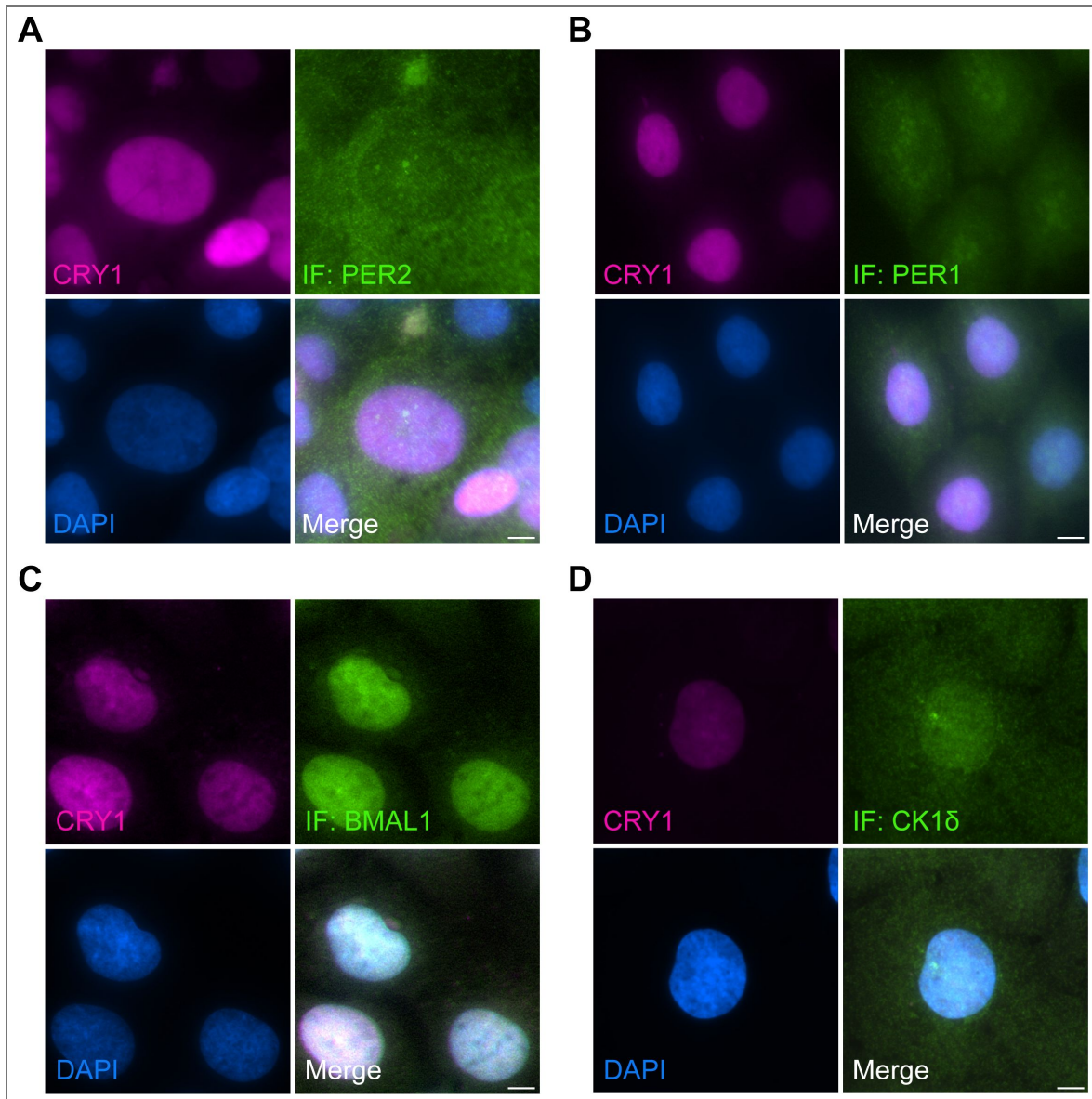


Fig EV2. Analysis of untransfected U2OStx_mK2-CRY1 cells for control of PER2 transfected cells shown in [Figure 2](#)

Untransfected U2OStx_mK2-CRY1 cells displays predominantly homogeneous nuclear localization of mK2-CRY1 and (A) cytoplasmic and nuclear localization of endogenous PER2. (B) cytoplasmic and slightly enriched nuclear localization of endogenous PER1. (C) nuclear localization of endogenous BMAL1. (D) diffuse nuclear and cytoplasmic localization of endogenous CK1δ as well as localization at the centrosome. Scale bars 10 μ m. n = 3.

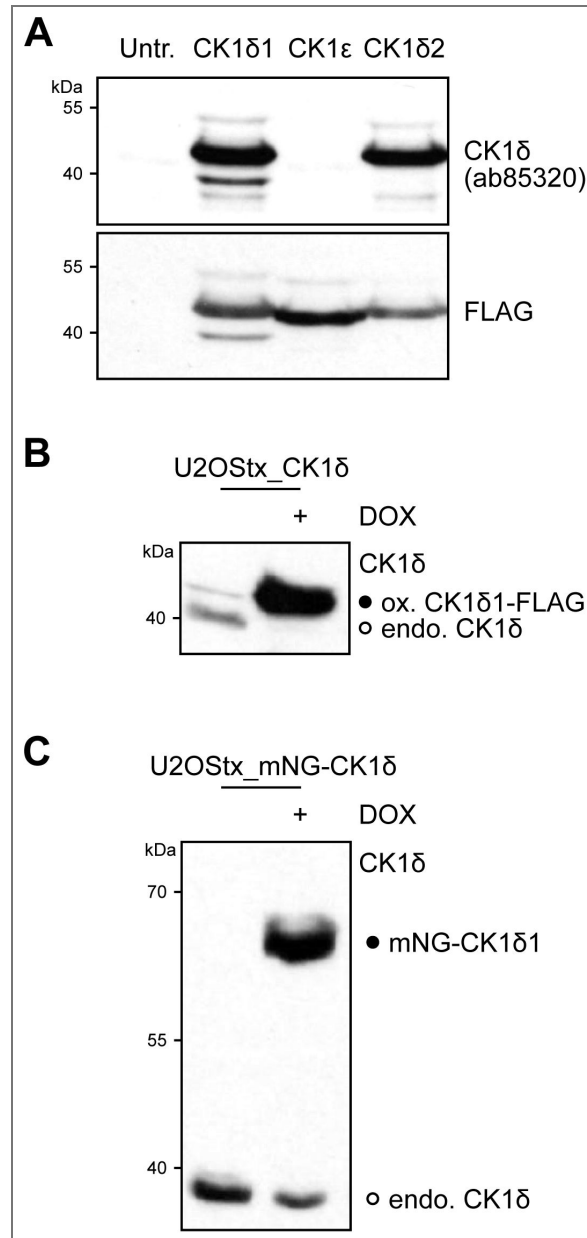


Fig EV3. Endogenous CK1δ levels decrease upon overexpression of transgenic CK1δ

(A) CK1δ antibody (abcam, Cat# ab85320) recognizes CK1δ1 and CK1δ2 but not CK1ε. FLAG-tagged kinases were expressed in HEK293T cells. Untr.: untransfected control. Cell lysates were analyzed by Western-blot with antibody ab85320 (upper panel) and FLAG antibody (lower panel). n = 3. (B) Overexpression of CK1δ1-FLAG and (C) mNG-CK1δ1 reduce expression levels of endogenous CK1δ. Western blots with CK1δ antibody ab85320. n = 3.

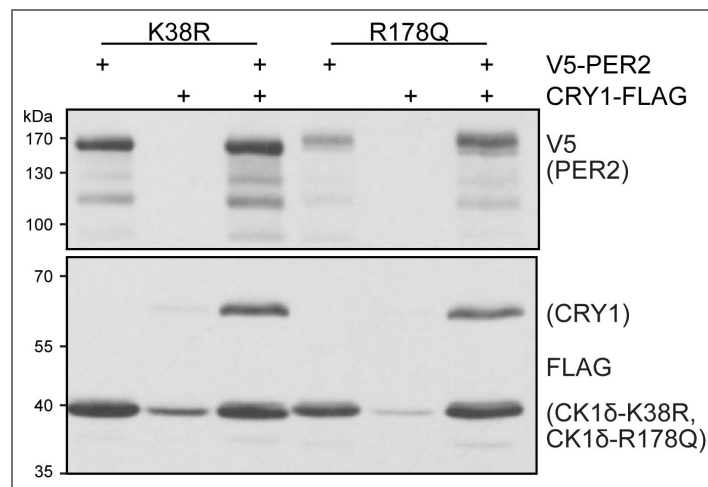


Fig EV4. PER2 supports stabilization of mutant kinases

PER2 stabilizes CRY as well as CK1δ1-K38R and CK1δ1-R178Q, which are in absence of PER2 already more stable than CK1δ1 (see Fig 4c, from the same blot). HEK293T cell expression of indicated combinations of V5-PER2 and FLAG-tagged mK2CRY1, CK1δ1-K38R and CK1δ1-R178Q. n = 3.

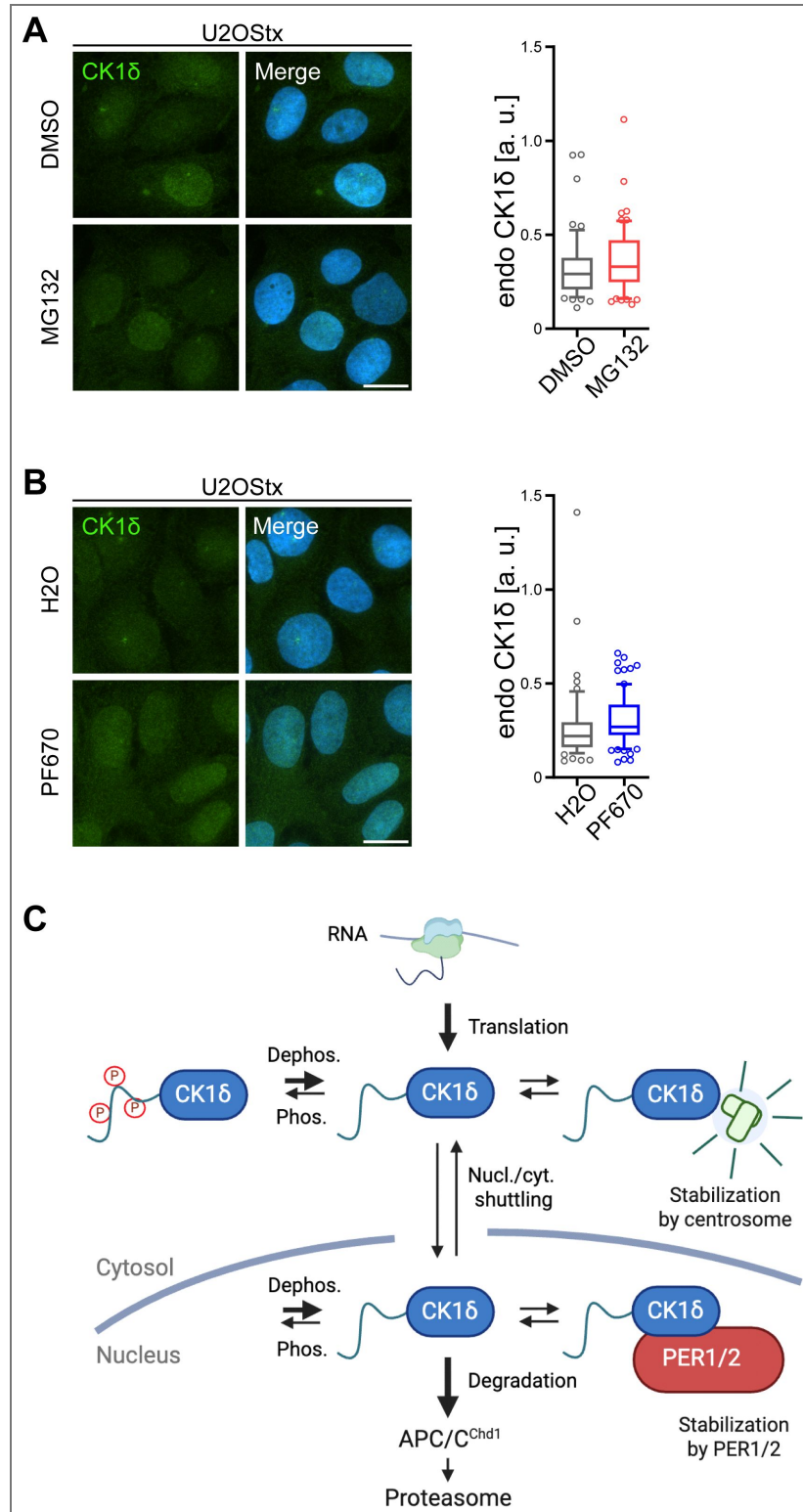


Fig EV5. Impact of proteasome inhibition and kinase inhibition on endogenous CK1δ abundance and localization

(A) Proteasome inhibition by 5 μM MG132 for 4 h and (B) Kinase inhibition by 1 μM PF670 for 1 h does not result in accumulation of endogenous CK1δ. Scale bars 20 μm. Right figure parts: Quantifications of (A) and (B) show no significant change in abundance of endogenous CK1δ in inhibitor-treated cells compared to the vehicle control. $n \geq 50$ cells, mean \pm SD. (C) Schematic of CK1δ homeostasis. For details see main text.

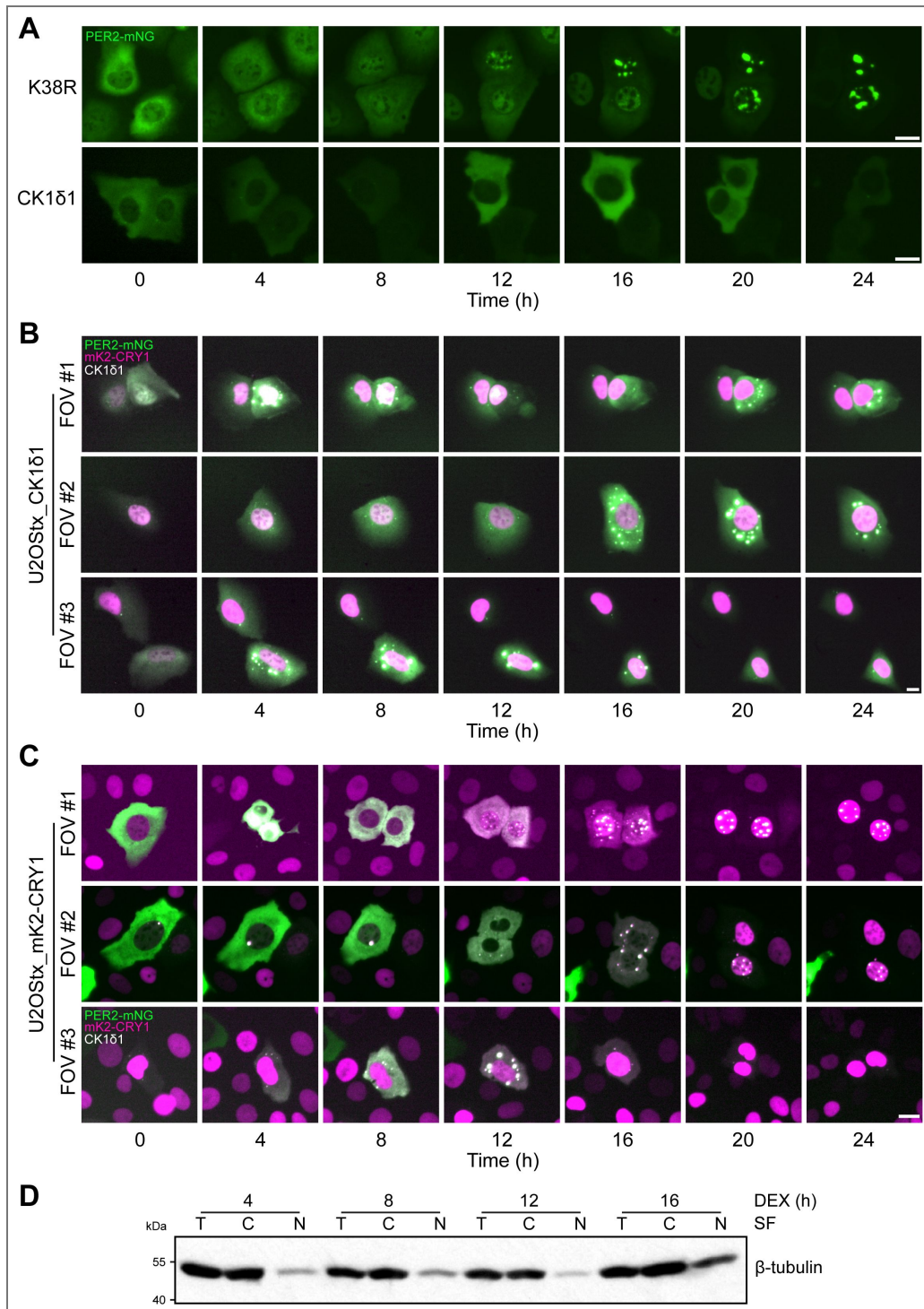


Fig EV6. Active CK1δ promotes the formation of cytoplasmic PER2:CRY1 foci, serving as reservoirs for CRY1 release into the nucleus

(A) PER2-mNG alone accumulates slowly in the nucleus when expressed with inactive CK1δ-K38R and in the cytoplasm when expressed with active CK1δ. *n* = 3. (B) Relates to Fig 6A. Additional fields of view showing cytoplasmic PER:CRY foci in U2OStx_CK1δ1 cells transfected with PER2-mNG and mK2-CRY1. (C) Relates to Fig 6D. Additional fields of view showing that cytoplasmic PER2-CRY1 foci serve as a reservoir for the CK1δ1-dependent release of mK2-CRY1 into the nucleus after degradation of PER2-mNG. Scale bars 20 μm. (D) Relates to Fig 6F. β-tubulin was used as a loading and fractionation control.

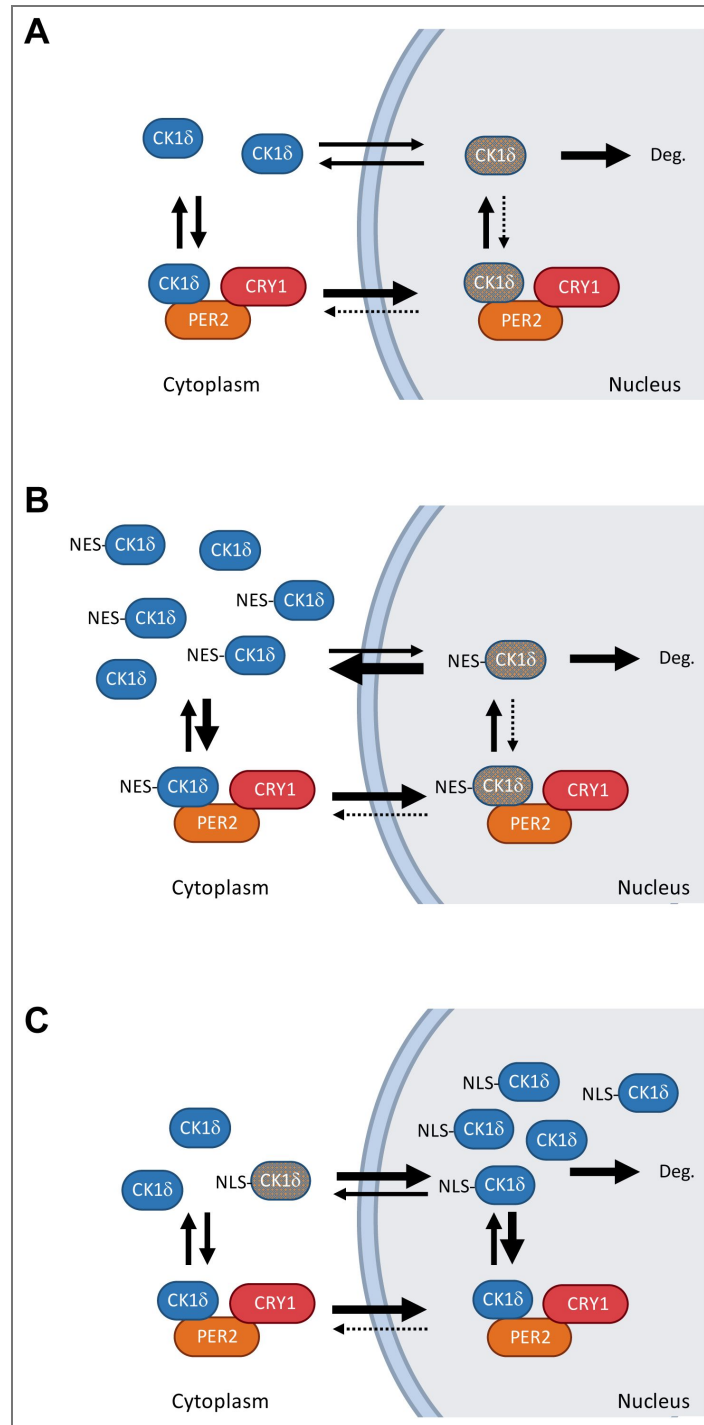


Fig EV7. Model illustrating the impact of nuclear and cytoplasmic CK1δ on circadian period length.

(A) Endogenous CK1δ continuously shuttles between the cytoplasm and the nucleus. Nuclear CK1δ levels remain low because the kinase is either rapidly degraded in the nucleus or efficiently exported back to the cytoplasm in a kinase activity-dependent manner. (B) Overexpression of NES-tagged CK1δ does not increase the nuclear kinase pool. The NES-tagged kinase enters the nucleus via PER:CRY complexes, with each PER molecule capable of importing only one NES-tagged kinase. Within the nucleus, PER-bound CK1δ equilibrates with the free nuclear pool. Once released from PER, rebinding of NES-tagged CK1δ is antagonized by either degradation or rapid export to the cytoplasm. Consequently, the nuclear kinase concentration remains low, and circadian period length is unaffected by NES-CK1δ overexpression. (C) Overexpression of NLS-tagged CK1δ increases the nuclear kinase pool by counteracting both nuclear export and degradation of CK1δ. This leads to a shortening of period length, as the elevated nuclear CK1δ facilitates PER2 binding and phosphorylation. Blue and gray schematic representations of CK1δ indicate high and low kinase concentrations, respectively.

Data availability

The data supporting the findings of this study are available within the article and its supplementary information files. This study includes no data deposited in external repositories. Plasmids and cell lines generated in this study are available from the lead contact, Michael Brunner (michael.brunner@bzh.uni-heidelberg.de) with a completed materials transfer agreement.

Acknowledgements

We thank Alessia Ruggieri und Michael Knop for providing mKATE-2 and mNeonGreen templates, respectively. This work was supported by the Deutsche Forschungsgemeinschaft, TRR186.

Additional information

Funding

Funder	Grant reference number	Author
Deutsche Forschungsgemeinschaft (DFG)	TRR 186	Michael Brunner

Author ORCID iDs

Fidel E Serrano: <https://orcid.org/0000-0001-8906-9343>

Daniela Marzoll: <https://orcid.org/0000-0002-8137-1991>

Axel CR Diernfellner: <https://orcid.org/0000-0001-6560-2318>

Michael Brunner: <https://orcid.org/0000-0001-9798-3047>

References

1. Takahashi J. S (2017) Transcriptional architecture of the mammalian circadian clock. *Nat Rev Genet* **18**:164-179 <https://doi.org/10.1038/nrg.2016.150> | PubMed
2. Partch C. L (2020) Orchestration of Circadian Timing by Macromolecular Protein Assemblies. *Journal of Molecular Biology* **432**:3426-3448 <https://doi.org/10.1016/j.jmb.2019.12.046> | PubMed
3. Lee C., Etchegaray J.-P., Cagampang F. R. A., Loudon A. S. I., Reppert S. M (2001) Posttranslational Mechanisms Regulate the Mammalian Circadian Clock. *Cell* **107**:855-867 [https://doi.org/10.1016/s0092-8674\(01\)00610-9](https://doi.org/10.1016/s0092-8674(01)00610-9) | PubMed
4. Bell-Pedersen D., et al. (2005) Circadian rhythms from multiple oscillators: lessons from diverse organisms. *Nat Rev Genet* **6**:544-556 <https://doi.org/10.1038/nrg1633> | PubMed
5. Partch C. L., Green C. B., Takahashi J. S (2014) Molecular architecture of the mammalian circadian clock. *Trends in Cell Biology* **24**:90-99 <https://doi.org/10.1016/j.tcb.2013.07.002> | PubMed
6. Preitner N., et al. (2002) The Orphan Nuclear Receptor REV-ERBa Controls Circadian Transcription within the Positive Limb of the Mammalian Circadian Oscillator. *Cell* **110**:251-260 [https://doi.org/10.1016/s0092-8674\(02\)00825-5](https://doi.org/10.1016/s0092-8674(02)00825-5) | PubMed
7. Sato T. K., et al. (2004) A Functional Genomics Strategy Reveals Rora as a Component of the Mammalian Circadian Clock. *Neuron* **43**:527-537 <https://doi.org/10.1016/j.neuron.2004.07.018> | PubMed
8. Ramsey K. M., Marcheva B., Kohsaka A., Bass J. (2007) The Clockwork of Metabolism. *Annu. Rev. Nutr* **27**:219-240 <https://doi.org/10.1146/annurev.nutr.27.061406.093546> | PubMed
9. Dibner C., Schibler U., Albrecht U (2010) The Mammalian Circadian Timing System: Organization and Coordination of Central and Peripheral Clocks. *Annu. Rev. Physiol* **72**:517-549 <https://doi.org/10.1146/annurev-physiol-021909-135821> | PubMed

10. Mohawk J. A., Green C. B., Takahashi J. S (2012) Central and Peripheral Circadian Clocks in Mammals. *Annu. Rev. Neurosci* **35**:445-462 <https://doi.org/10.1146/annurev-neuro-060909-153128> | PubMed
11. Cao X., Wang L., Selby C. P., Lindsey-Boltz L. A., Sancar A (2023) Analysis of mammalian circadian clock protein complexes over a circadian cycle. *Journal of Biological Chemistry* **299**:102929 <https://doi.org/10.1016/j.jbc.2023.102929> | PubMed
12. Koike N., et al. (2012) Transcriptional Architecture and Chromatin Landscape of the Core Circadian Clock in Mammals. *Science* **338**:349-354 <https://doi.org/10.1126/science.1226339> | PubMed
13. Ye R., et al. (2014) Dual modes of CLOCK:BMAL1 inhibition mediated by Cryptochrome and Period proteins in the mammalian circadian clock. *Genes Dev* **28**:1989-1998 <https://doi.org/10.1101/gad.249417.114> | PubMed
14. Chiou Y.-Y., et al. (2016) Mammalian Period represses and de-represses transcription by displacing CLOCK-BMAL1 from promoters in a Cryptochrome-dependent manner. *Proc. Natl. Acad. Sci. U.S.A* **113** <https://doi.org/10.1073/pnas.1612917113> | PubMed
15. Aryal R. P., et al. (2017) Macromolecular Assemblies of the Mammalian Circadian Clock. *Molecular Cell* **67**:770-782.e6 <https://doi.org/10.1016/j.molcel.2017.07.017> | PubMed
16. Michael A. K., et al. (2017) Formation of a repressive complex in the mammalian circadian clock is mediated by the secondary pocket of CRY1. *Proc. Natl. Acad. Sci. U.S.A* **114**:1560-1565 <https://doi.org/10.1073/pnas.1615310114> | PubMed
17. Fribourgh J. L., et al. (2020) Dynamics at the serine loop underlie differential affinity of cryptochromes for CLOCK:BMAL1 to control circadian timing. *eLife* **9**:e55275 <https://doi.org/10.7554/eLife.55275> | PubMed
18. Smyllie N. J., et al. (2025) Quantitative measures of clock protein dynamics in the mouse suprachiasmatic nucleus extends the circadian time-keeping model. *EMBO J* **44**:3614-3644 <https://doi.org/10.1038/s44318-025-00426-z> | PubMed
19. Brunner M (2025) CRYing for balance: a repressor lingers through peak circadian transcription. *EMBO J* **44**:3550-3552 <https://doi.org/10.1038/s44318-025-00467-4> | PubMed
20. Bae K., et al. (2001) Differential Functions of mPer1, mPer2, and mPer3 in the SCN Circadian Clock. *Neuron* **30**:525-536 [https://doi.org/10.1016/s0896-6273\(01\)00302-6](https://doi.org/10.1016/s0896-6273(01)00302-6) | PubMed
21. Zheng B., et al. (2001) Nonredundant Roles of the mPer1 and mPer2 Genes in the Mammalian Circadian Clock. *Cell* **105**:683-694 [https://doi.org/10.1016/s0092-8674\(01\)00380-4](https://doi.org/10.1016/s0092-8674(01)00380-4) | PubMed
22. Griffin E. A., Staknis D., Weitz C. J (1999) Light-Independent Role of CRY1 and CRY2 in the Mammalian Circadian Clock. *Science* **286**:768-771 <https://doi.org/10.1126/science.286.5440.768> | PubMed
23. Horst G. T. J. V. D., et al. (1999) Mammalian Cry1 and Cry2 are essential for maintenance of circadian rhythms. *Nature* **398**:627-630 <https://doi.org/10.1038/19323> | PubMed
24. Fustin J.-M., et al. (2018) Two *Ck1δ* transcripts regulated by m6A methylation code for two antagonistic kinases in the control of the circadian clock. *Proc. Natl. Acad. Sci. U.S.A* **115**:5980-5985 <https://doi.org/10.1073/pnas.1721371115> | PubMed
25. Lee H., Chen R., Lee Y., Yoo S., Lee C (2009) Essential roles of CKIδ and CKIε in the mammalian circadian clock. *Proc. Natl. Acad. Sci. U.S.A* **106**:21359-21364 <https://doi.org/10.1073/pnas.0906651106> | PubMed
26. Landgraf D., Wang L. L., Diemer T., Welsh D. K (2016) NPAS2 Compensates for Loss of CLOCK in Peripheral Circadian Oscillators. *PLoS Genet* **12**:e1005882 <https://doi.org/10.1371/journal.pgen.1005882> | PubMed
27. Toh K. L., et al. (2001) An hPer2 Phosphorylation Site Mutation in Familial Advanced Sleep Phase Syndrome. *Science* **291**:1040-1043 <https://doi.org/10.1126/science.1057499> | PubMed
28. Vanselow K., et al. (2006) Differential effects of PER2 phosphorylation: molecular basis for the human familial advanced sleep phase syndrome (FASPS). *Genes Dev* **20**:2660-2672 <https://doi.org/10.1101/gad.397006> | PubMed

29. Philpott J. M., et al. (2023) PERIOD phosphorylation leads to feedback inhibition of CK1 activity to control circadian period. *Molecular Cell* **83**:1677-1692.e8 <https://doi.org/10.1016/j.molcel.2023.04.019> | PubMed
30. Zhou M., Kim J. K., Eng G. W. L., Forger D. B., Virshup D. M (2015) A Period2 Phosphoswitch Regulates and Temperature Compensates Circadian Period. *Molecular Cell* **60**:77-88 <https://doi.org/10.1016/j.molcel.2015.08.022> | PubMed
31. Narasimamurthy R., et al. (2018) CK1 δ/ϵ protein kinase primes the PER2 circadian phosphoswitch. *Proc. Natl. Acad. Sci. U.S.A* **115**:5986-5991 <https://doi.org/10.1073/pnas.1721076115> | PubMed
32. Philpott J. M., et al. (2020) Casein kinase 1 dynamics underlie substrate selectivity and the PER2 circadian phosphoswitch. *eLife* **9**:e52343 <https://doi.org/10.7554/eLife.52343> | PubMed
33. Hornbeck P. V., et al. (2015) PhosphoSitePlus, 2014: mutations, PTMs and recalibrations. *Nucleic Acids Research* **43**:D512-D520 <https://doi.org/10.1093/nar/gku1267> | PubMed
34. Marzoll D., et al. (2022) Casein kinase 1 and disordered clock proteins form functionally equivalent, phospho-based circadian modules in fungi and mammals. *Proc. Natl. Acad. Sci. U.S.A* **119**:e2118286119 <https://doi.org/10.1073/pnas.2118286119> | PubMed
35. Vielhaber E., Eide E., Rivers A., Gao Z.-H., Virshup D. M (2000) Nuclear Entry of the Circadian Regulator mPER1 Is Controlled by Mammalian Casein Kinase I ϵ . *Mol Cell Biol* **20**:4888-4899 <https://doi.org/10.1128/mcb.20.13.4888-4899.2000> | PubMed
36. Schitteck B., Sinnberg T (2014) Biological functions of casein kinase 1 isoforms and putative roles in tumorigenesis. *Mol Cancer* **13**:231 <https://doi.org/10.1186/1476-4598-13-231> | PubMed
37. Cruciat C.-M (2014) Casein kinase 1 and Wnt/ β -catenin signaling. *Current Opinion in Cell Biology* **31**:46-55 <https://doi.org/10.1016/j.ceb.2014.08.003> | PubMed
38. Smyllie N. J., et al. (2016) Visualizing and Quantifying Intracellular Behavior and Abundance of the Core Circadian Clock Protein PERIOD2. *Current Biology* **26**:1880-1886 <https://doi.org/10.1016/j.cub.2016.05.018> | PubMed
39. Smyllie N. J., et al. (2022) Cryptochrome proteins regulate the circadian intracellular behavior and localization of PER2 in mouse suprachiasmatic nucleus neurons. *Proc. Natl. Acad. Sci. U.S.A* **119**:e2113845119 <https://doi.org/10.1073/pnas.2113845119> | PubMed
40. Öllinger R., et al. (2014) Dynamics of the circadian clock protein PERIOD2 in living cells. *Journal of Cell Science jcs* 156612 <https://doi.org/10.1242/jcs.156612> | PubMed
41. Gabriel C. H., et al. (2021) Live-cell imaging of circadian clock protein dynamics in CRISPR-generated knock-in cells. *Nat Commun* **12**:3796 <https://doi.org/10.1038/s41467-021-24086-9> | PubMed
42. Gabriel C. H., et al. (2024) Circadian period is compensated for repressor protein turnover rates in single cells. *Proc. Natl. Acad. Sci. U.S.A* **121**:e2404738121 <https://doi.org/10.1073/pnas.2404738121> | PubMed
43. Xie P., et al. (2023) Mammalian circadian clock proteins form dynamic interacting microbodies distinct from phase separation. *Proc. Natl. Acad. Sci. U.S.A* **120**:e2318274120 <https://doi.org/10.1073/pnas.2318274120> | PubMed
44. Guillen R. X., Beckley J. R., Chen J.-S., Gould K. L (2020) CRISPR-mediated gene targeting of CK1 δ/ϵ leads to enhanced understanding of their role in endocytosis via phosphoregulation of GAPVD1. *Sci Rep* **10**:6797 <https://doi.org/10.1038/s41598-020-63669-2> | PubMed
45. Yagita K., et al. (2002) Nucleocytoplasmic shuttling and mCRY-dependent inhibition of ubiquitylation of the mPER2 clock protein. *The EMBO Journal* **21**:1301-1314 <https://doi.org/10.1093/emboj/21.6.1301> | PubMed
46. Smyllie N. J., et al. (2022) Cryptochrome proteins regulate the circadian intracellular behavior and localization of PER2 in mouse suprachiasmatic nucleus neurons. *Proc. Natl. Acad. Sci. U.S.A* **119**:e2113845119 <https://doi.org/10.1073/pnas.2113845119> | PubMed
47. Xing W., et al. (2013) SCFFBXL3 ubiquitin ligase targets cryptochromes at their cofactor pocket. *Nature* **496**:64-68 <https://doi.org/10.1038/nature11964> | PubMed

48. Nangle S. N., et al. (2014) Molecular assembly of the period-cryptochrome circadian transcriptional repressor complex. *eLife* **3**:e03674 <https://doi.org/10.7554/eLife.03674> | PubMed
49. Badura L., et al. (2007) An Inhibitor of Casein Kinase I ϵ Induces Phase Delays in Circadian Rhythms under Free-Running and Entrained Conditions. *J Pharmacol Exp Ther* **322**:730-738 <https://doi.org/10.1124/jpet.107.122846> | PubMed
50. Cheong J. K., et al. (2011) IC261 induces cell cycle arrest and apoptosis of human cancer cells via CK1 δ/ϵ and Wnt/ β -catenin independent inhibition of mitotic spindle formation. *Oncogene* **30**:2558-2569 <https://doi.org/10.1038/onc.2010.627> | PubMed
51. Penas C., et al. (2015) Casein Kinase 1 δ Is an APC/CCdh1 Substrate that Regulates Cerebellar Granule Cell Neurogenesis. *Cell Reports* **11**:249-260 <https://doi.org/10.1016/j.celrep.2015.03.016> | PubMed
52. Okamura H., et al. (2004) A Conserved Docking Motif for CK1 Binding Controls the Nuclear Localization of NFAT1. *Mol Cell Biol* **24**:4184-4195 <https://doi.org/10.1128/mcb.24.10.4184-4195.2004> | PubMed
53. Milne D. M., Looby P., Meek D. W (2001) Catalytic Activity of Protein Kinase CK1 δ (Casein Kinase 1 δ) Is Essential for Its Normal Subcellular Localization. *Experimental Cell Research* **263**:43-54 <https://doi.org/10.1006/excr.2000.5100> | PubMed
54. Sillibourne J. E., Milne D. M., Takahashi M., Ono Y., Meek D. W (2002) Centrosomal Anchoring of the Protein Kinase CK1 δ Mediated by Attachment to the Large, Coiled-coil Scaffolding Protein CG-NAP/AKAP450. *Journal of Molecular Biology* **322**:785-797 [https://doi.org/10.1016/s0022-2836\(02\)00857-4](https://doi.org/10.1016/s0022-2836(02)00857-4) | PubMed
55. Greer Y. E., et al. (2014) Casein kinase 1 δ functions at the centrosome and Golgi to promote ciliogenesis. *MBoC* **25**:1629-1640 <https://doi.org/10.1091/mbc.e13-10-0598> | PubMed
56. Elmore Z. C., Guillen R. X., Gould K. L (2018) The kinase domain of CK1 enzymes contains the localization cue essential for compartmentalized signaling at the spindle pole. *MBoC* **29**:1664-1674 <https://doi.org/10.1091/mbc.e18-02-0129> | PubMed
57. Fung H. Y. J., Fu S.-C., Brautigam C. A., Chook Y. M (2015) Structural determinants of nuclear export signal orientation in binding to exportin CRM1. *eLife* **4**:e10034 <https://doi.org/10.7554/eLife.10034> | PubMed
58. Cunha B. A., Sibley C. M., Ristuccia A. M (1982) Doxycycline. *Therapeutic Drug Monitoring* **4**:115
59. Cao X., Yang Y., Selby C. P., Liu Z., Sancar A (2021) Molecular mechanism of the repressive phase of the mammalian circadian clock. *Proc. Natl. Acad. Sci. U.S.A* **118**:e2021174118 <https://doi.org/10.1073/pnas.2021174118> | PubMed
60. Lu J., et al. (2021) Types of nuclear localization signals and mechanisms of protein import into the nucleus. *Cell Commun Signal* **19**:60 <https://doi.org/10.1186/s12964-021-00741-y> | PubMed
61. Gallego M., Eide E. J., Woolf M. F., Virshup D. M., Forger D. B (2006) An opposite role for *tau* in circadian rhythms revealed by mathematical modeling. *Proc. Natl. Acad. Sci. U.S.A* **103**:10618-10623 <https://doi.org/10.1073/pnas.0604511103> | PubMed
62. Lowrey P. L., et al. (2000) Positional Syntenic Cloning and Functional Characterization of the Mammalian Circadian Mutation *tau*. *Science* **288**:483-491 <https://doi.org/10.1126/science.288.5465.483> | PubMed
63. Meng Q.-J., et al. (2008) Setting Clock Speed in Mammals: The CK1 ϵ *tau* Mutation in Mice Accelerates Circadian Pacemakers by Selectively Destabilizing PERIOD Proteins. *Neuron* **58**:78-88 <https://doi.org/10.1016/j.neuron.2008.01.019> | PubMed
64. Vielhaber E. L., Duricka D., Ullman K. S., Virshup D. M (2001) Nuclear Export of Mammalian PERIOD Proteins. *Journal of Biological Chemistry* **276**:45921-45927 <https://doi.org/10.1074/jbc.m107726200> | PubMed
65. Narumi R., et al. (2016) Mass spectrometry-based absolute quantification reveals rhythmic variation of mouse circadian clock proteins. *Proc. Natl. Acad. Sci. U.S.A* **113** <https://doi.org/10.1073/pnas.1603799113> | PubMed

66. Park J., Lee K., Kim H., Shin H., Lee C (2023) Endogenous circadian reporters reveal functional differences of *PERIOD* paralogs and the significance of PERIOD:CK1 stable interaction. *Proc. Natl. Acad. Sci. U.S.A* **120**:e2212255120 <https://doi.org/10.1073/pnas.2212255120> | PubMed
67. Rey G., et al. (2011) Genome-Wide and Phase-Specific DNA-Binding Rhythms of BMAL1 Control Circadian Output Functions in Mouse Liver. *PLoS Biol* **9**:e1000595 <https://doi.org/10.1371/journal.pbio.1000595> | PubMed
68. Hoffmann J., et al. (2014) Non-Circadian Expression Masking Clock-Driven Weak Transcription Rhythms in U2OS Cells. *PLoS ONE* **9**:e102238 <https://doi.org/10.1371/journal.pone.0102238> | PubMed
69. Brown S. A., et al. (2008) Molecular insights into human daily behavior. *Proc. Natl. Acad. Sci. U.S.A* **105**:1602-1607 <https://doi.org/10.1073/pnas.0707772105> | PubMed

Peer reviews

Reviewer #2 (Public review):

Summary:

This study aims to examine the effects of the subcellular localization of the mammalian clock protein PER2 and its dedicated binding partners CRY1 and the kinase CK1. Using a combination of transient transfection and a Dox-inducible expression system, they show that CRY1 promotes nuclear retention of PER2, and that phosphorylation of PER2 by CK1 promotes cytoplasmic localization and release of CRY1. Changes in complex assembly and subcellular localization could impact the transcriptional repressive function of the CK1-PER2-CRY1 complex in the molecular clock.

Strengths:

The study establishes a system of transient transfection and Dox-inducible expression that allows for strict temporal control of the presence of fluorescently-tagged clock proteins. This is essential to conduct time-lapse microscopy studies that determine changes in the apparent subcellular localization and stability of associated clock proteins. With the potential caveats of overexpression set aside, the authors make use of good controls and supplement cell-based work with in vitro experiments where possible. The discovery that phosphorylation of PER2 by CK1 in the nucleus leads to cytoplasmic localization of PER2 and PER2-CRY1 complexes is a new finding. Moreover, the apparent dissociation of CRY1 from PER2 after CK1 phosphorylation provides a potentially new mechanism by which the repressive activity of this complex could be regulated.

Weaknesses:

Overexpression of circadian clock components, normally expressed at low levels, could disrupt the stoichiometry of native interactions, Although the authors provide a reasonable rationale for the Dox-inducible approach and use appropriate controls throughout the experiments, there is still concern that overexpression of the components of this transcriptional repressive complex far exceed the concentration of the transcription factor they regulate, and this has not been taken into consideration here. In addition, the interesting discovery that CK1 phosphorylation of PER2 leads to dissociation of CRY1 has not identified the phosphorylation site(s) responsible for this, so the mechanism by which this occurs is still unknown. Still, this study provides some interesting hypotheses regarding CK1 regulation of PER2 and CRY1 that could drive future work in the field.

Comments on latest version:

This manuscript has already undergone two rounds of review at a reputable journal, and we have been provided with the previous reviewers' comments and the authors' responses. I am satisfied with the responses and changes to the manuscript made in these previous rounds of review and don't have any further experiments to suggest that wouldn't represent significant additional work.

<https://doi.org/10.7554/eLife.110786.1.sa1>

Author response:

[These author responses are to reviews from another journal.]

Reviewer #1:

This manuscript investigates the behaviour of a variety of clock proteins in cultured cells when epitope tagged and transiently expressed and try to draw general implications for endogenous function of circadian clock proteins.

Clock proteins are expressed at low levels in most cells, and so the clock interacting proteins (other kinases, phosphatases, ubiquitin-conjugated enzymes, etc.) are likewise probably at low abundance. Over-expression of one or two or even three components of a multicomponent system is going to produce odd and obscure non-physiological imbalances. The authors do not extend detailed study of these imbalances to more physiologic levels so the importance of their observations to clock function is not clear, and importantly, they are not tested in more biologically relevant models.

To study the function of components within a system, the steady state must be perturbed in one way or another. This can be achieved through pharmacological treatment, mutagenesis, downregulation, or overexpression. Such interventions are inherently non-physiological, and the relevance of the resulting observations must therefore be carefully validated.

In our study, the purpose of PER2 overexpression was to investigate its subcellular dynamics in the absence and presence of CRYs, specifically CRY1. This is far less trivial than it might appear at first glance, because our data clearly show that PER2 overexpression triggers, within 24 h, the accumulation of endogenous CRY1 (Fig. 1A), due to PER2-mediated stabilization of CRY1 (Fig. 4). PER2 overexpression also induces the accumulation of endogenous PER1, CK1, and BMAL1 (Fig. 2).

This effect was not considered in previous studies, such as Yagita et al. (2002), in which PER2 subcellular localization was assessed at a single time point following transient transfection. Yagita et al. found roughly equal proportions of cells with PER2 exclusively in the nucleus, exclusively in the cytoplasm, or distributed between both compartments. Such extreme cell-to-cell variability cannot be explained solely by PER2's shuttling dynamics, as that would imply synchronous export in one cell and synchronous import in another.

Our time-resolved analysis of DOX-induced PER2 expression strongly suggests that the variability reported by Yagita et al. reflects a heterogeneous population of unsynchronized cells at different temporal stages along a trajectory from cytoplasmic PER2 (unbound) to nuclear PER2 fully saturated with CRYs (bound), owing to stabilization of endogenous CRYs. Similarly, Öllinger et al. (2014) analyzed PER2 nuclear export in cells constitutively expressing PER2-Dendra. Under such steady-state conditions, PER2-Dendra is already in complex with endogenous CRYs. The slow export rate and lack of dependence on additional CRY1 expression therefore likely reflect export of the complex, which is intrinsically slow.

Thus, prior to our work, no data on the true shuttling dynamics of PER2 were available.

Importantly, our results show not only that CRY1 promotes nuclear accumulation of PER2 (as reported by Öllinger et al.) but also that, conversely, PER2 promotes cytosolic accumulation of CRY1, depending on their expression ratio. Since CRY1 is predominantly nuclear and PER2 predominantly cytosolic, and because a PER2 dimer can bind one or two CRY1 molecules, our data suggest that the shuttling equilibrium depends on PER2 saturation state: a PER2 dimer bound to one CRY1 remains cytosolic, whereas a dimer bound to two CRY1 is nuclear.

These observations are novel and have not been reported previously. They were only possible through time-resolved analysis of overexpressed proteins.

A number of the findings are confirmatory rather than novel - the phosphorylation-regulated nuclear-cytoplasmic shuttling of CK1 and PER proteins is long known, and it's not clearly stated what is novel here.

We acknowledge prior work by Milne et al. (2001), who showed that kinase-dead CK1 is predominantly nuclear and that prolonged treatment with leptomycin B (16 h) enhances its nuclear localization. We cite this study at the beginning of the relevant paragraph. While we confirm these earlier observations, our work extends them in several important and novel ways:

(1) Rapid dynamics of CK1 localization – We show that pharmacological inhibition of CK1 with PF670 induces rapid (within 1 h) depletion of CK1 δ from the centrosome, accompanied by nuclear accumulation and elevated CK1 δ levels. These kinetics have not previously been reported. We also show that proteasome inhibition with MG132 enhance centrosomal staining, indicating that centrosomal binding sites are not saturated. Together, the data show that CK1 δ equilibrates rapidly between its binding partners.

(2) Integration of localization with protein stability – We relate the known localization patterns of WT CK1 and the kinase-dead mutant K38R to CK1 degradation dynamics and further compare them to the tau-like kinase mutant CK1 δ -R1178Q. This integration of subcellular localization data with turnover mechanisms provides new mechanistic insight.

(3) Comprehensive regulatory model – In the revised manuscript, we now include a schematic summarizing how CK1 δ is posttranslationally regulated via subcellular shuttling, nuclear degradation, and dynamic interactions with binding partners (Figure EV5C). To our knowledge, such a comprehensive view of CK1 δ regulation, linking localization, stability, and partner association, has not been presented before.

We believe these additions clearly distinguish our findings from prior reports and highlight the novel aspects of our study.

The formation of PER and CRY and CK1 complexes likewise is well established. The finding that formation of multiprotein complexes stabilize otherwise unstable over-expressed proteins is interesting but not novel.

We fully agree that the existence of PER–CRY–CK1 complexes is well established. It is also known that PER2 stabilizes CRY1 by occupying the FBXL3 binding site and that CRY1 promotes the nuclear accumulation of PER2. We do not present these established interactions as novel findings.

Our novel contribution, as outlined above, is the discovery that the shuttling and subcellular localization of PER2 and CRY1 are mutually dependent on their expression ratio. Specifically, we show for the first time that the steady-state shuttling distribution PER2 alone is cytosolic due to its rapid nuclear export whereas CRY1 is predominantly nuclear (known). Given that CRY1 facilitates the nuclear import of PER2 (known) and that a PER2 dimer can bind either one or two CRY1 molecules, our data showing that cytoplasmic PER2-CRY1 foci contain less

CRY1 than nuclear foci lead us to conclude that cytoplasmic PER2 complexes contain one CRY1 molecule, while nuclear complexes contain two.

This model provides a mechanistic explanation for the distribution of PER2 between the cytosol and nucleus and for the relatively lower cytosolic CRY1 levels. Most importantly, we further show (for the first time) that CK1-mediated phosphorylation of PER2 displaces CRY1. This phosphorylation event would produce PER2 dimers with one or no CRY1 bound, promoting their export to the cytosol. We believe this represents a novel and potentially important mechanism for regulating circadian clock function.

The results from many of the imaging assays are not quantitated, and the figures often show single cells. It's hard to draw statistical significance from these.

The phenotypes we report here are result of multiple technical and biological replicates (n >3). Image analysis and statistical analysis was performed when required. We show additional examples in the EVs.

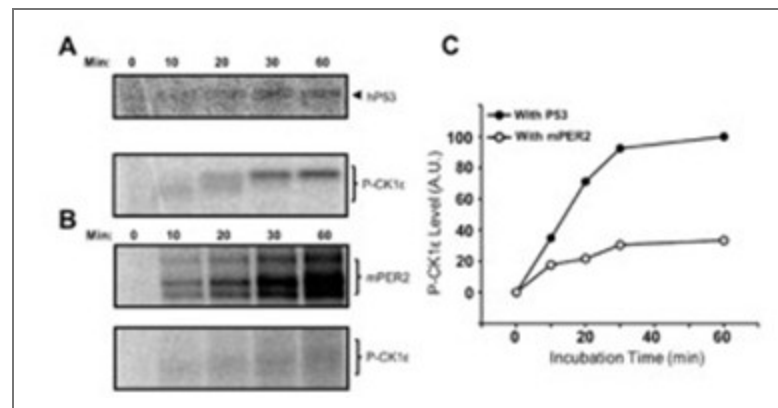
There are a number of phenomena seen whose physiological relevance is unclear. In figure 1, forced over-expression of CRY1 and PER2 leads to formation of nuclear foci. It is unlikely these foci form at non-overexpressed levels, and so the general interest and relevance is not high nor investigated. This reduces the impact of the finding.

It has been shown that PERs and CRYs do not form thermodynamically stable, large (detectable) foci under physiological conditions, as we have stated in the manuscript. Whether these proteins have the propensity to form smaller, more dynamic structures of physiological relevance is an interesting question that could be explored elsewhere, but it is not relevant to our study. In our work, these foci are simply convenient markers for analyzing the interaction and subcellular (co)localization of clock proteins under investigation. In the revised version, we have kept the analysis of these foci and the discussion of their potential relevance to a minimum in order to avoid confusion and unnecessary discussions.

The finding that CK1 δ is kept in the dephosphorylated state by binding to PER has been established previously by Johnson and colleagues and should perhaps be mentioned (Qin JBR 2015 (doi: 10.1177/0748730415582127)).

There is clearly a misunderstanding here. Qin et al.'s data show that, in a cell-free system, CK1 ϵ phosphorylates PER2 and also autophosphorylates its C-terminal tail (autoradiograph, Fig. 1E).

However, because PER2 phosphorylation is carried out by CK1 ϵ that is tightly anchored to PER2, there is competition between PER2 phosphorylation and tail autophosphorylation. As a result, the kinetics of tail phosphorylation are slower (Fig. 3B and quantification in C) than those observed with free CK1 ϵ (as seen in the presence of the p53 substrate, Fig. 3A,C). We believe that this is also happening in the cell.



Author response image 1.

Our data, in contrast, address a different point. It has been known from the Virshup lab for decades that CK1 δ/ϵ undergo futile cycles of (auto)phosphorylation and dephosphorylation, resulting in an active, dephosphorylated kinase in cells because cellular phosphatases are more efficient than CK1 autophosphorylation. We now show that CK1 δ is also efficiently dephosphorylated when bound to PER2 (Fig. 3). Nevertheless, despite dephosphorylation of PER2-bound CK1 δ , PER2 itself becomes hyperphosphorylated, indicating that cellular phosphatases act differently on these two substrates. To clarify this point, we inhibited phosphatases with calyculin A (CalA). Under these conditions, both PER2 and PER2-bound CK1 δ became efficiently hyperphosphorylated (new Fig. 3).

The degradation of kinase-active but not inactive CK1 is only shown here with 50-fold overexpressed protein so it's interesting, but the relevance to circadian biology is not made clear. The fact that over-expressed CK1 is degraded primarily in the nucleus is interesting, but needs further characterization - is this affected by the epitope tag? Is it true of endogenous CK1 or only over-expressed CK1? Is this not seen with e.g. other forms of CK1, e.g. lacking the C-terminus?

The observation that unassembled kinase is rapidly degraded is most clearly demonstrated by overexpression experiments. However, Fig. 3 shows that overexpression of CRY1 and PER2 leads to the accumulation of elevated levels of endogenous CK1 δ (untagged), indicating that endogenous kinase is likewise degraded in the absence of a stabilizing binding partner. In addition, we present data showing that overexpression of tagged CK1 δ reduces the levels of endogenous, untagged CK1 δ , further supporting the conclusion that unassembled endogenous CK1 δ is unstable and subject to degradation.

Further characterization of the CK1 degradation pathway is of considerable interest and could form the basis of a separate study, particularly to identify the components that mediate activity-dependent nuclear export and activity-dependent nuclear degradation. The Δ -tail kinase is expressed at very low levels, although interpretation is complicated by the possibility that this reflects pleiotropic effects.

The final figure, showing that nuclear CK1 is the form responsible for shortening rhythms, is interesting. Is this because massive increases in nuclear CK1 alter PER, or BMAL/CLOCK, or proteasome activity?

Our data show that cells expressing either nuclear or cytosolic CK1 are viable, proliferate normally, and maintain a functional circadian clock. Therefore, overexpression of the kinase does not produce pleiotropic effects.

To assume it's due to PER phosphorylation is in disagreement with the studies of Meng et al. Neuron 2008 DOI 10.1016/j.neuron.2008.01.019.

The data are not in disagreement with Meng et al.; in fact, they align quite well. Meng et al. showed that CK1 ϵ -tau shortens the circadian period, which we had also previously reported for CK1 δ -tau-like (Marzoll et al., 2022). We now demonstrate that CK1 δ tau-like is enriched in the nucleus, contributing to its period-shortening phenotype. Furthermore, we show that active CK1 δ (but not CK1 δ -K38R) promotes cytoplasmic accumulation of PER:CRY complexes, consistent with PER2 degradation in the cytosol as described by Meng et al.

Taken together, these findings suggest that PER proteins acquire their CK1 in the nucleus, and this interaction determines the circadian period length. Following a time delay—set by the kinetics of PER2 phosphorylation—PER2:CRY complexes are exported to the cytosol along with their bound CK1, where they are subsequently degraded.

Reviewer #2:

Interactions between the circadian clock proteins PER1/2 with CK1d/e and CRY1/2 influence each of their stability, subcellular localization, and activity, as countless studies over the last two decades have shown. However, many questions still remain, especially in light of newer models of the transcription-translation feedback loop (TTFL) in which the repression phase relies on two distinct mechanisms, a phosphorylation-dependent displacement of the transcription factor by CK1-PER-CRY complexes from DNA early in repression, and a CRY1 dependent sequestration of the transcription factor activation domain later in repression. In particular, questions remain about mechanisms triggering nuclear entry/export and activity of these proteins in the cytoplasm and nucleus.

Here, the authors utilize a system of induced and/or transient overexpression of proteins with or without with fluorophores to track subcellular localization, stability, and interactions. As the authors point out throughout the manuscript, the overexpression of these clock proteins often causes them to behave differently from the endogenous proteins. It looks as though the authors have done their best to account for these changes, and they have certainly been rigorous in pointing them out, but there is concern that some of the conclusions may be influenced by this overexpression. For example, the relevance of work related to the overexpression-dependent foci is unclear.

Same answer as to Reviewer 1: It has been shown that PERs and CRYs do not form thermodynamically stable, large (detectable) foci under physiological conditions, as we have stated in the manuscript. Whether these proteins have the propensity to form smaller, more dynamic structures of physiological relevance is an interesting question that could be explored elsewhere, but it is not relevant to our study. In our work, these foci are simply convenient markers for analyzing the interaction and subcellular (co)localization of the clock proteins under investigation. In the revised version, we have kept the analysis of these foci and the discussion of their potential relevance to a minimum in order to avoid confusion.

The findings that the stability of the kinase depend on localization, its intrinsic activity, and interaction with PER2 are interesting and important. Use of the CKBD deletion to show that CK1 stabilization depends on its anchoring interaction with PER2 is a nice touch. The authors bring up an excellent point that most of the potential phosphorylation sites on PER1 and PER2 have not been functionally characterized aside from the phosphoswitch mechanism. Their observation that CK1 eventually induces cytoplasmic localization of the CK1-PER-CRY1 complex and the release of CRY1 is intriguing. In particular, the finding that pretreatment of PER2 with CK1 in vitro blocked its ability to interact with CRY1 is very interesting. However, the absence of mechanistic data to explore this in more detail limits the impact of this conclusion. Using the system they have established here to identify the site(s) on PER2 and/or CRY1 that lead to this would help to solidify this work and increase the impact of this work. Overall, there are some

interesting findings here but the inclusion of some competing viewpoints and mechanistic data would strengthen the impact of the work.

Major

(1) The characterization of the tau-like CK1 mutant R178C as less active than the wild type enzyme is not entirely correct—it is less active on the FASP region as described, but it has increased activity on S478 in the phosphodegron that is independent of inhibition from the FASP region (Gallego et al. PNAS, 2007 and Philpott et al. eLife, 2020). It is still possible that some of the period shortening effects of the mutant could arise from enhanced nuclear accumulation, but the oversimplified description of the mutant as less active should be corrected.

In the revised version, we discuss that the enhanced nuclear localization of the Tau-like kinase may contribute, at least in part, to period shortening, similar to how forced nuclear overexpression of wild-type kinase also shortens the period. We emphasize, however, that CK1 Tau is compromised in its priming-dependent activity, whereas its priming-independent activity is context-specific and enhanced toward the β -TrCP site.

(2) One of main conclusions from the paper, that CK1 induces cytoplasmic localization of the CK1-PER2-CRY1 complex and subsequent release of CRY1 would be strengthened significantly by identifying the phosphorylation site(s) responsible for the cytoplasmic localization of the complex and the release of CRY1. The system they have developed here seems ideal to identify these sites.

We fully agree with the reviewer. We substituted the known phosphorylation sites in PER2 surrounding the CRY-binding domain, but this had no effect on the phosphorylation-dependent release of CRY1. Therefore, a more systematic analysis will be required, including the possibility that phosphorylations in CRY1 itself may contribute. To this end, we are generating PER2 and CRY1 variants in which all Ser/Thr residues are replaced by Ala. Using these constructs alongside the wild-type versions, we will by PCR systematically create hybrids in which specific regions containing phosphorylation sites are exchanged.

Nevertheless, this will require considerable time and effort, and we believe this investigation exceeds the scope of the present manuscript and will address it in future work.

(3) The concept of delayed release of CRY1 presented here is an interesting one. It's unclear why the authors have also not incorporated prior findings (Ukai-Tadenuma et al. Cell, 2012, Koike et al. Science, 2012) that peak levels of CRY1 are expressed in a later phase than CRY2, PER1, and PER2. It seems like figure EV6 should reflect the observation that CRY2 is the predominant cryptochrome present during early repression (Koike et al. Science, 2012).

The reviewer is absolutely right: the expression phases of CRY1, CRY2, PER1, and PER2 are important. I have recently discussed these issues in detail in a News & Views article in The EMBO Journal, commenting on a paper by Smyllie et al. In this News & Views article, I discuss that the presently available data suggest that CRY1 is always present throughout the circadian cycle and keeps circadian transcription partially repressed even at peak phases of expression. In the revised version, I refer to these publications, including those mentioned by the reviewer. However, I would like to keep the model presented in the supplementary figure as simple as possible and specifically focused on the work presented in this manuscript, rather than presenting a comprehensive conceptual model of the circadian clock.

(4) The model presented in figure EV6 and described throughout the text shows that PER-CRY complexes interact with CK1 in the nucleus, and not in the cytoplasm prior to nuclear entry. Prior work on endogenous protein complexes has shown that CK1-PER-CRY

complexes exist in the cytoplasm very early on in the repression phase (Aryal et al. Mol Cell, 2017-ref. 14 in the manuscript). Work by Sancar and colleagues (Cao et al. PNAS, 2020) also shows with endogenous proteins that CK1 δ has a circadian pattern of nuclear entry (or possibly retention) concomitant with PER2 that is dependent on the presence of PERs and CRYs. Together, these data seem to be inconsistent with your model.

We think the data are not inconsistent. The recent Smyllie et al. paper in *EMBO Journal* shows that PER2 is present in both the cytosol and the nucleus at all times when it is expressed, but cytosolic PER2 is not saturated with CRY, which is more nuclear. Our data demonstrate that PER2 shuttles between the cytosol and the nucleus depending on its occupancy with CRYs (see schematic Fig. 1). Occupancy, in turn, depends on expression levels and binding affinities, including those of CRY2 and PER1. Consequently, PER2 complexes could shuttle continuously throughout the circadian cycle—either because they are not saturated with CRYs due to the balance between expression levels, freely available CRY, and binding affinity, or later in the cycle because CRYs are displaced by phosphorylation. If PER2 acquires casein kinase in the nucleus early in the cycle, it will shuttle out to the cytosol together with the bound CK1. We believe this does occur, but early in the circadian cycle the saturation of PER2 with casein kinase is likely to be very low due to the limited availability of CK1 in the nucleus. I am aware that not everyone will share this interpretation point by point, but discussing it in greater length and detail exceeds the scope of the present manuscript.

Reviewer #3:

This manuscript by Serrano and co-workers is a tight body of work that provides much needed insights into the regulation of clock proteins by CK1D, and into the regulation of CK1D itself. While the whole paper relies on artificial overexpression of chimeric/tagged proteins that may have significant differences in the function, the stability and subcellular distribution of the endogenous proteins they are suppose to model, this limitation was been clearly stated by the authors, and nevertheless their study still provides important insights.

While the authors have specified which Ck1d isoform (Ck1d1) they are overexpressing in their model cell lines, they may have thought to consider that the overexpression of one Ck1 homologue may affect the endogenous expression of the other homologues and their isoforms, e.g. ck1d1 overexpression may cause an increase in Ck1d2 or Ck1e, which would in turn affect the conclusions.

We show in revised Fig. 3 that overexpression of CK1 δ 1 reduces the expression of endogenous CK1 δ 1/2. This is consistent with our prediction that overexpressed and endogenous CK1 (including CK1 ϵ) compete for the same stabilizing binding partners, leading to rapid degradation of unassembled kinases.

Moreover, the antibody they used for endogenous Ck1d (which is ab85320, also mentioned as AF12G4 but that is the clone number, not the catalogue number) is discontinued and its specificity against Ck1d1, Ck1d2 or even the highly identical Ck1e, has not been clearly demonstrated. We know from Fig 3 that it can detect Ck1d1 but it would be great if the authors would provide additional evidence for the specificity of this antibody, for example by overexpressing Ck1d1/Ck1d2/Ck1e to see really which "endogenous" Ck1 we are seeing.

Are the three bands for example seen in Fig 4A corresponding to the different isoforms? This simple experiment would reinforce the conclusions.

We show in the revised figure that the antibody recognizes CK1 δ 1 and CK1 δ 2, but not CK1 ϵ . In U2OS cells, the antibody detects a single band (Figure); we do not know whether this represents predominantly one splice isoform or both, which are not resolved. However, this

distinction is not relevant for our interpretation, because overexpression of tagged CK1 δ 1 reduces the expression of whichever endogenous kinase is present.

There are no minor comments, as the figures, the figure legends and main text are all of good quality and ready for publication.

Reviewers' Responses to Point-by-Point Response to Peer Review

Referee #1:

I appreciated the additional efforts by the authors to improve the manuscript. Unfortunately, the underlying approach of forced over-expression remains artifact-prone, and has been largely supplanted by readily available knockin and targeted mutagenesis methods. Over-expression may give clues, but I think more rigorous mechanistic validation is needed to make this compelling. I cannot support publication of this manuscript.

Referee #2:

In their response to reviewers, the authors make the valid point that the steady state of a system is usually perturbed to study it. In this study, they have used overexpression of the clock proteins PER2, CRY1 and CK1 to study their effects on subcellular dynamics and stability. In justifying this choice, they refer to several papers that similarly overexpressed at least one of these components, stating that their time-resolved approach brings novel insights. However, there is a missed opportunity here to translate any lessons learned from overexpression studies to a system where the proteins are expressed at physiological levels and stoichiometry.

The authors reply to reviewer 1 stating that they conclude PER proteins acquire CK1 in the nucleus, but this does not account for other studies showing an apparent PER-CK1 complex in the cytoplasm during the early phases of repression and/or a pattern of PER-dependent nuclear entry of CK1 (Lee et al. 2001, Cell; Aryal et al. 2017 Mol Cell; Cao et al. 2021 PNAS). Given that all 3 of these studies were done with native expression levels, it seems incumbent upon the authors to demonstrate that their conclusions from the overexpression study are physiologically relevant by translating them in some way to a more native system. This also addresses a point made by reviewer 2, major concern 4 that was not satisfactorily addressed by the authors. Perhaps they could validate their hypothesis of PER shuttling and interactions with CK1 or CRY1 that alter this in a native system similar to Aryal or Cao et al. with the use of nuclear export inhibitors?

The response to reviewer 2, major concern 1 is thoughtful and much appreciated. However, simplifying the effects of the tau mutation on CK1 as having a decreased rate on priming-dependent phosphorylation but not priming-independent is not quite true—the tau mutation also decreases the rate of priming-independent phosphorylation of S662 (in humans) (Philpott et al. 2020, eLife).

Other papers appearing in this journal seem to all include at least one major new mechanistic insight. Although the authors do a diligent job in characterizing the overexpressed proteins in this system, some of their conclusions are at odds with prior studies of the system in more native conditions, so the potential impact of this work is unclear. To verify these conclusions or test new ones (ie, that CK1 disrupts PER-CRY1 interactions), they should use their insights to generate mutations or make perturbations in a native system and demonstrate that they still hold.

Referee #3:

The authors have adequately addressed the reviewers' comments, and it is my opinion that the manuscript is ready for publication. It is true, as previously mentioned by other

reviewers, that the evidence presented rely on overexpression, which for the other reviewers seem to preclude publication. However, I find this to be a too strict opinion.

If the authors had indeed provided evidence using crispr-cas9-mediated genetic manipulation and tagging/mutating endogenous genes for all their experiments, thereby providing more physiological evidence of how clock proteins interact, they would probably have submitted their manuscript to an alternative journal with a higher impact.

As it stands, it is my opinion that, considering the evidence and limitations of the study, this manuscript is a good match for the journal.

Author Rebuttal:

Apologies for the delayed reply regarding our manuscript. In the meantime, we have added several new experiments which address the comments of the reviewers and more. These are now included as Figures 1C, EV3, 4D, 6E, 6F, EV6D, and EV7.

Figure 1C reinforces our observations from Figure 1B showing that induction of stably-integrated PER2 also results in accumulation of endogenous CRY1 at a timescale that is compatible with the gradual localization of overexpressed PER2 into the nucleus.

Figure EV3 addresses several technical comments from Reviewers #3 and #1, respectively: Figure EV3A shows that our CK1 δ antibody recognizes CK1 δ 1 and CK1 δ 2, but not CK1 ϵ . Figures EV 3B and C clearly show how overexpression of our transgenic CK1 δ results in decreased endogenous CK1 δ which further demonstrates the rapid turnover of active kinase.

Figure 4D addresses the comment from Reviewer #2. We clearly show that CK1 δ is not kept in a dephosphorylated state by binding to PER. In addition to our direct comment to this point, Figure 4D shows that CK1 δ regardless if it is expressed alone or in complex with PER2 is phosphorylated to a similar extent when the cells are treated with the phosphatase inhibitor CalA. As indicated in our direct response, we are rather more interested in the observation that cellular phosphatases act differently on PER2 compared to CK1 δ despite being in the same PER:CK1 δ complex (as shown by the clear stabilization of overexpressed CK1 δ by co-expression of PER2).

Figures 6E, 6F, and EV6D demonstrate that our observations from overexpression systems are also observed in a more physiological context, addressing comments from Reviewers #1 and #2. Figure 6E shows that dephosphorylation of PER2 leads to its relocalization from the cytosol to the nucleus, while Figure 6F analyzes the subcellular localization of PER2 in the context of a functional circadian clock in U2OS cells. The latter demonstrates that PER2 is predominantly nuclear early in the circadian cycle, but redistributes to the cytosol at later time points. We included these experiments in response to the reviewer's request for a more physiological context. Since we are not a mouse lab, this cell-based system represents the most physiological model we can provide. Figure 6F show the dynamics of endogenous PER2 from DEX-synchronized cells. At early timepoints, PER2 is predominantly nuclear likely due to the incorporation of CRY1 forming the PER:CRY complex. At later timepoints PER2 is redistributed between the cytoplasm and nucleus due to PER2 phosphorylation. Importantly, these results are consistent with and recontextualize the results from Liu et al. (Xie et al., PNAS, 2023) showing the hypophosphorylated PER2 at early timepoints post-DEX is predominantly nuclear and hyperphosphorylated PER2, that appear later post-DEX is predominantly cytoplasmic.

Finally, Figure EV7 provides a model how the subcellular distribution of CK1 δ affects its assembly into the PER:CRY complex emphasizing how nuclear kinase enacts its role in the circadian clock.

Response to Reviewers:

We were disappointed by the categorical rejection of overexpression experiments. Without a specific discussion of why they would be inappropriate or not sufficient in the context of the work presented here, the blanket assertion that overexpression inevitably produces artifacts

functions more as a rhetorical device than as a substantiated scientific argument. The fact that the term ‘physiological’ generally carries a positive connotation, whereas ‘overexpression’ is often perceived negatively, does not in itself justify the categorical rejection of experiments.

While we appreciate that some reviewers may personally prefer alternative strategies, we believe that the suitability of any approach must be evaluated in light of the specific biological questions being addressed. I cannot see a single specific point in the reviewers’ responses indicating that any of our experiments yielded artificial results. It is true that targeted knock-in and mutagenesis methods are available, however, these approaches are simply not suited to the questions raised in this manuscript. We also fully agree that, whenever possible, insights from overexpression studies should be validated in systems with a functional clock where proteins are expressed at physiological levels, which we did using U2OS cells, and noting the compatibility of our results with those in the literature using endogenously-tagged constructs. We have cited several recent studies that have investigated the subcellular distribution and circadian dynamics of endogenous or endogenously-tagged clock proteins in mice (Cao et al, 2021; Smyllie et al, 2022, 2016, 2025) and U2OS cells (Öllinger et al, 2014; Gabriel et al, 2021; Xie et al, 2023). While we cannot substantially expand on these previous observations, we confirm them in the revised version by demonstrating the nuclear-to-cytoplasmic relocalization of PER2 in U2OS cells over the course of a circadian cycle. In addition, we show that this process is, in principle, reversible: when CK1 is inhibited with PF670, overexpressed hyperphosphorylated cytosolic PER2 becomes dephosphorylated and accumulates in the nucleus.

Overall, we consider our approach not only complementary but also essential, as it enables us to address two key questions that would otherwise be difficult or even impossible to resolve:

(1) Mutual impact of PER2 and CRY1 on subcellular dynamics and the role of PER2 phosphorylation

Evidence from mouse liver (Cao et al, 2021), mouse SCN (Smyllie et al, 2022, 2025), and U2OS cells (Xie et al, 2023) indicates that a substantial fraction of PER2 remains cytoplasmic throughout its expression cycle, even in the presence of CRY1, which promotes PER’s nuclear import. The mechanisms underlying this cytoplasmic retention remain unclear, and no circadian function has yet been attributed to the cytosolic PER2 pool. Our study addresses how PER2 abundance, phosphorylation state, and stoichiometry relative to CRY1 govern their interaction and subcellular dynamics. This is physiologically relevant because PER1/2 and CRY1/2 proteins oscillate in expression and degradation out of phase, such that their concentrations, stoichiometry, and phosphorylation state vary systematically over the circadian cycle. Transient transfection and inducible overexpression combined with time-lapse microscopy are essential here, as they uniquely allow modulation of protein ratios and CK1 δ levels and to resolve their dynamics.

Previous work established that CRY1 is nuclear and promotes PER2 nuclear accumulation (Smyllie et al, 2022). Our data extend this by showing that subcellular distribution is determined by the CRY1:PER2 ratio. While CRY1 alone is nuclear we show that PER2 alone is cytoplasmic due to rapid nuclear export. Mixed conditions reveal ratio-dependent shifts: at low CRY1-to-PER2 ratios, CRY1 relocalizes to the cytoplasm, whereas at high ratios, PER2 is retained in the nucleus. We explain this behavior by PER2 dimerization: dimers bound to two CRY1 molecules remain nuclear, while dimers bound to a single CRY1 localize to the cytosol. Such species can be expected to form in a physiological context depending on binding affinities and rhythmic expression levels and ratios across circadian time. Importantly, we show that CK1 δ -mediated phosphorylation destabilizes PER2 and CRY1 interactions. From this, we infer that PER2 dimers with only a single bound CRY1 transiently form and accumulate in the cytosol, consistent with the lower CRY1-to-PER2 ratio we observe in the cytosol and that has also been reported in the SCN (Smyllie et al, 2025). With continued phosphorylation, PER2 dimers lose CRY1 altogether, while the released CRY1 accumulates in the nucleus. We suggest that this mechanism supports and extends the late repressive phase

of the circadian cycle. Recent data show that hypophosphorylated PER2 is predominantly nuclear, whereas hyperphosphorylated PER2 is largely cytoplasmic in mouse liver (Cao et al, 2021; Xie et al, 2023), linking our data to a physiological context.

Taken together, these findings suggest a mechanism whereby stoichiometry, subunit composition, and CK1 δ phosphorylation determine PER:CRY complex composition and localization. Crucially, these complexes and their dynamic relocalization could only be observed using inducible overexpression; knock-in strategies at endogenous levels would not be able to capture such states.

(2) Posttranslational regulation and subcellular homeostasis of CK1 δ and impact on the clock

Previous work has shown that nuclear export of CK1 δ depends on its kinase activity (Milne et al, 2001). Here, we further demonstrate that unassembled CK1 δ is subject to degradation, with nuclear turnover accelerated by its catalytic activity. Thus, when evaluating the impact of CK1 δ mutants on the circadian clock, one must consider not only kinase activity but also protein stability and subcellular distribution. We find that CK1 δ availability for PER2 differs between cytosol and nucleus. In particular, nuclear CK1 δ is limiting, and its abundance directly determines circadian period length. This is significant because subcellular CK1 δ availability and posttranslational regulation have not previously been examined or incorporated into circadian clock models, as the kinase has been assumed to be non-limiting given its constant expression throughout the circadian cycle. Complex formation between CK1 δ and PER is a well-established determinant of circadian timing, with CK1 δ overexpression known to shorten period length. Our data explain why: the binding equilibrium between CK1 δ and PER must be finely tuned. Previous studies suggested that PER associates with CK1 δ in the cytosol and enters the nucleus as a PER:CRY:CK1 δ complex (Lee et al, 2001; Aryal et al, 2017). Our data suggest that nuclear PER is not saturated with CK1 δ . This is because levels of free, active CK1 δ in the nucleus are low, owing to its rapid export or degradation by the nuclear proteasome, which limits its availability for PER binding.

Our overexpression studies support this mechanism. NES-tagged CK1 δ overexpression does not alter circadian period length, because it fails to increase nuclear CK1 δ levels: Each PER molecule can coimport only one kinase, a process already occurring in wild-type cells, and the few co-imported molecules rapidly equilibrate with the nuclear pool, where they are subject to export or degradation. In contrast, NLS-tagged CK1 δ overexpression directly increases nuclear kinase abundance by antagonizing export, thereby enhancing PER binding and shortening circadian period. This multilayered regulation of CK1 δ stability and localization and its consequences for PER2 availability would not have been revealed without targeted overexpression. Our findings therefore fill a key knowledge gap and remain fully consistent with previous studies (Lee et al, 2001; Aryal et al, 2017; Cao et al, 2021).

Conclusion: In sum, our findings are novel and physiologically relevant, aligning with data from mouse liver and SCN. While studies at strictly endogenous protein levels are important and necessary, perturbation of steady state is a standard strategy to uncover and observe novel mechanisms. Endogenous-level experiments would demand technically unrealistic systems (for example, even the simplest case, analyzing the subcellular dynamics of PER2 alone, would require cells lacking PER1, CRY1/2, and CK1 δ/ϵ). Moreover, adjustment of PER2-to-CRY1 ratios cannot be achieved with stably integrated genes and of course not at physiological expression levels. Thus, inducible overexpression is not merely practical but currently the most feasible approach to dissect these dynamics. We complement our findings with data from U2OS cells with a functional clock, showing that the availability of nuclear CK1 δ directly determines circadian period length. Although specific aspects of our extended model require further experimental validation, no published evidence contradicts it to date. Mechanistic discussions of the circadian clock have so far focused primarily on PER protein degradation. Our model broadens this perspective by incorporating CK1 δ homeostasis, PER:CRY complex composition, subcellular localization, and their regulation by phosphorylation. In doing so, it provides a detailed framework to be critically tested and refined in future studies.

<https://doi.org/10.7554/eLife.110786.1.sa0>